surface antigen of foetal/adult hepatic stem/progenitor cells.

It has become clear that tumour, in many cases, is a heterogeneous cell population and only a small fraction of the cells possess the potential to self-renew. Cancer stem cell or tumour initiating cell, which was first documented in haematological malignancies, has subsequently been discovered in many solid tumours, including breast, brain, prostate, liver, lung, melanoma, pancreas and colon tumours (*32–36*). While it was shown that CD133, known as a stem cell marker, is expressed in cancer stem cells in many tumours including HCC (*37–41*), the relation between normal tissue stem cells and cancer stem cells is not clear in most of the cases.

In this study, we established many hybridoma clones which produced anti-hDlk-1 monoclonal antibodies (mAb). Among them, we selected three independent clones usable for immunohistochemistry and characterized these antibodies by flow cytometry. Using these mAbs which recognized a different epitope, we investigated the expression of human Dlk-1 (hDlk-1) during liver development by immunohistochemistry. The expression of hDlk-1 showed a pattern similar to mouse Dlk-1 during liver development, suggesting that hDlk-1 is also a marker of hepatic stem/progenitor cells in embryo. We then examined hDlk-1 expression in human neoplastic liver lesions. About a half of HCC specimens from under 40-years-old patients expressed hDlk-1, whereas the positive ratio of hDlk-1 over 50-years-old patients was ~10%. Our study indicates the possibility that hDlk-1 is a common cell surface antigen both in human foetal liver stem/progenitor cells and in a part of HCC. Moreover, hDlk-1 was also frequently expressed in colon, breast, pancreas and lung carcinoma. These observations suggest that hDlk-1 is a potential target for monoclonal antibody-based therapy in those carcinomas.

Materials and Methods

Plasmid constructs

Full length hDlk-1 and its derivatives (EGF1-3 and EGF 4-6) were amplified by PCR. The sequences of primers were as follows: Fw1: 5′-cgcgtccgcaaccagaagccc-3′, Rv1: 5′-aagcttgatctcctcgtcgccggcc-3′ (for full length hDlk-1), Fw2: 5′-gcggccgcgctgaatgcttcccggcc-3′, Rv2: tctagaggcccgaacatctctatcac-3′ (for hDlk-1 EGF1-3), Fw3: 5′-gcggccgcgcctgctcctcggccccc-3′, Rv3: 5′-gcgtatagtaagctctgcgg-3′ (for hDlk-1 EGF4-6). All PCR products were verified by DNA sequencing. Full-length hDlk-1 cDNA was cloned in pcDNA3 vector (Invitrogen, Carlsbad, CA) with Flag tag. hDlk-1 EGF1-3 cDNA was subcloned in pME18SNeo carrying the signal sequence of CD8, His tag, and transmenbrane and cytoplasmic domains of FXYD5, which was kindly gifted by Dr Tanaka, M. (University of Tokyo, Tokyo, Japan). hDlk-1 EGF4-6 cDNA was subcloned in pME18SNeo containing the signal sequence of CD8, His tag.

Antibodies

Mouse monoclonal antibodies against hDlk-1 (clone DI-6, DI-2-20 and DI-4-22) were generated by the DNA immunization method (Nosan Corp., Kanagawa, Japan). To prepare purified monoclonal antibodies, hybridoma clones (3×10^6 cells) were intraperitoneally administered to BALB/c Slc-nu/nu mice (Japan SLC, Shizuoka, Japan), which received 2,6,10,14-tetramethylpentadecane (Sigma Aldrich Japan K.K., Tokyo, Japan) 7 days before injection of hybridoma. After collection of ascites, the antibodies were purified with a protein G column (GE Healthcare, Buckinghamshire, England). Rabbit polyclonal antibodies against hDlk-1 were prepared by immunizing with peptides containing the extracellular domain of hDlk-1 except for the putative signal sequence. Polyclonal antibodies were purified by affinity chromatography using columns conjugated with the peptides used for immunization.

Cell culture, transfection and flow cytometry

COS7 cells, HEK-293 cells, Huh-7 cells and SK-N-FI cells were maintained in Dulbecco's modified Eagle's medium (DMEM) supplemented with 10% foetal bovine serum. HepG2 cells and C3A/HepG2 cells were maintained in MEM supplemented with 10% foetal bovine serum. COS7, HEK-293, Huh-7 and HepG2 cells were from Human Science Research Resource Bank (Osaka, Japan). SK-N-FI and C3A/HepG2 cells were purchased from American Type Culture Collection (Rockville, MD). Transfection was performed using Lipofectoamine and Plus reagent (Invitrogen). To establish HEK-293 cells stably expressing hDlk-1 (293-hDlk-1), HEK-293 cells were transfected with pcDNA3 vector containing full-length hDlk-1 cDNA and selected with G418 (Invitrogen). COS7 cells were transiently transfected with expression constructs containing either hDlk-1 EGF1-3 or hDlk EGF4-6, and two days after transfection, these cells were harvested and subjected to fluorescence activated cell sorter (FACS) analysis. 293-hDlk-1 cells were cultured to subconfluency and harvested for flow cytometry by FACSCalibur (Nippon Becton Dickinson, Tokyo, Japan).

Immunohistochemistry

Tissue arrays and sections of tumours used in this study were purchased from Cybrdi (Rockville, MD), Shanghai Outdo Biotech Co. (Shanghai, China), Super Bio Chips (Seoul, Korea), ISU ABXIS (Seoul, Korea), US Biomax (Rockville, MD). Clinical information of patients (age, sex, grade and pathology diagnosis) is described in their homepage and data sheets. Foetal liver specimens were purchased from Biochain (Hayward, CA).

Paraffin embedded tissue sections and arrays were deparaffinized, and then autoclaved for 5 min in citrate buffer (pH 6.0) or TE buffer (pH 9.0). Slides were treated with methanol containing 0.3% H_2O_2 to inhibit endogenous peroxidase activity, and incubated with anti-hDlk-1 mAbs (10 μg/ml) at 4°C over night. After washing with phosphate-buffered saline (PBS), sections were stained with Vectastain ABC Elite kit (Vector, Burlingame, CA) and then counterstained with haematoxylin (Wako, Osaka, Japan). HCC sections with more than 10% immunopositive cells, either cell membrane or cytoplasmic stainin, were considered as positive.

Result

Characterization of anti-hDlk1 monoclonal antibodies

We established over 100 hybridoma clones producing anti-hDlk-1 mAb. Among them, three independent clones usable for immunohistochemistry in paraffin-embedded tissue sections were selected. First, we evaluated the reactivity and specificity of these antibodies by flow cytometry. Three mAbs against hDlk-1, DI-6, DI-2-20 and DI-4-22, specifically recognized HEK-293 cells stably expressing hDlk-1 (Fig. 1B), but not parent HEK-293 cells (not shown). On the other hand, these antibodies failed to recognize mouse Dlk-1, which shares ~90% similarity with hDlk-1 at the amino acid level (data not shown). These results confirmed that anti-hDlk-1 mAbs, DI-6, DI-2-20 and DI-4-22, specifically recognize hDlk-1. We then mapped the region of hDlk-1 to which the antibodies bind using deletion mutants of hDlk-1 (Fig. 1A). As shown in Fig. 1D, DI-6 recognized the EGF repeats 1–3 (amino acid 24–129), whereas DI-2-20 and DI-4-22 recognized EGF repeats 4–6 (amino acid 126–382). DI-2-20 and DI-4-22 recognized the same epitope because they competed each other (results not shown).

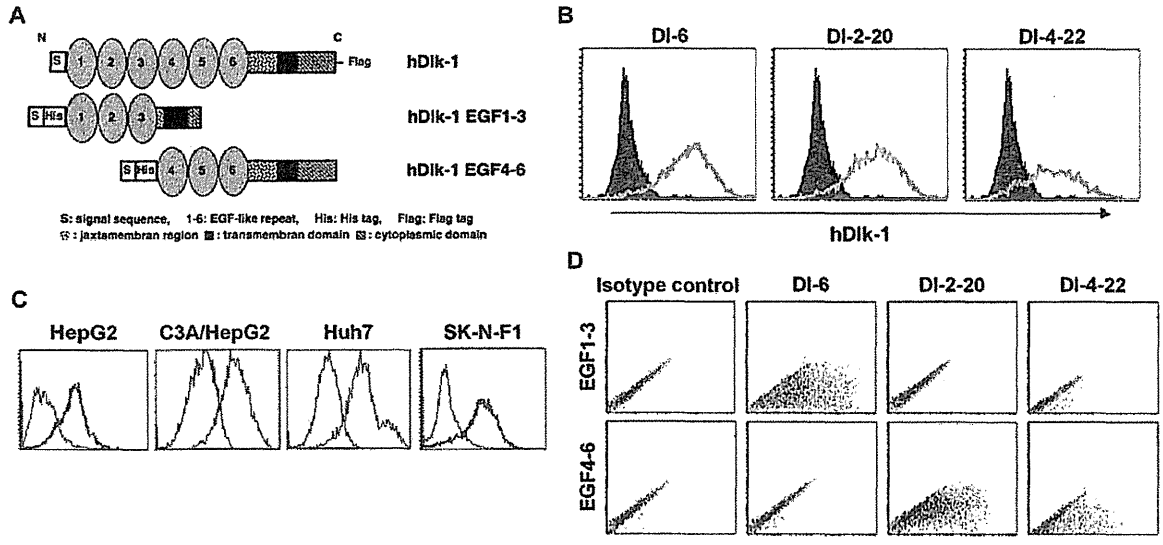

Fig. 1 Characterization of anti-hDlk-1 monoclonal antibodies by FACS analysis. (A) Schematic representation of various hDlk-1 constructs used in this study. (B) Three monoclonal antibodies used in this study specifically recognize hDlk-1 expressing cells. HEK-293 cells stably-expressing hDlk-1 were harvested, dispersed in a single cell suspension, and analysed by flow cytometry using monoclonal antibodies against hDlk-1, DI-6, DI-2-20, DI-4-22 (green line). Blue area: isotype control (mouse IgG1). (C) Anti-hDlk-1 mAb DI-2-20 also recognizes endogenous hDlk-1 in human cancer cell lines. Cancer cell lines indicated here were harvested and subjected to FACS analysis by using DI-2-20, respectively. Blue line: isotype control (mouse IgG1), red line: anti-hDlk-1 mAb (DI-2-20). Another monoclonal antibody, DI-6, showed similar result (data not shown). (D) Identification of the region of hDlk-1 to which anti-hDlk-1 mAbs bind. COS7 cells were transiently transfected with plasmids containing a various domain of hDlk-1 represented in (A). Two days after transfection, these cells were harvested and subjected to FACS analysis with anti-hDlk-1 mAb, DI-6, DI-2-20 and DI-4-22, respectively. DI-2-20 and DI-4-22 recognize EGF repeat 4–6, whereas DI-6 recognizes EGF repeat 1–3.

As reported previously, hDlk-1 was expressed early in liver development, but not in adult liver (*9*). To confirm that selected mAbs were suitable for immunohistochemistry in paraffin-embedded tissue sections, the expression pattern of hDlk-1 protein in liver was examined by immunohistochemical staining using DI-2-20 mAb (Fig. 2). A foetal liver tissue at 22 weeks (22w) showed membrane and cytoplasmic staining of hDlk-1 in hepatocytes. However, hDlk-1 was not detected in foetal liver at 38 weeks (38w) and adult liver. Northern blot analysis showed that hDlk-1 mRNA was strongly expressed in foetal liver from 6 to 12 weeks of gestation (not shown). The expression of hDlk-1 showed a pattern similar to mouse Dlk-1 during liver development, suggesting that hDlk-1 is also a marker of hepatic stem/progenitor cells in embryo. Similar results were obtained with either DI-6 or DI-4-22 mAb, though less sensitive than DI-2-20 (not shown). These results suggest that DI-2-20 was also useful for detecting endogenous hDlk-1 by immunohistochemistry. Therefore, we used mainly DI-2-20 mAb for further analysis.

Expression of hDlk-1 in HCC cells

We then examined the cell surface expression of hDlk-1 in a number of cancer cell lines originated from HCC by flow cytometry by using DI-6 and DI-2-20 antibodies. Among them, significant cell surface expression of hDlk-1 was detected in HepG2, C3A/HepG2 and Huh-7 cells (Fig. 1C). These results suggest that hDlk-1 is the cell surface antigen of HCC

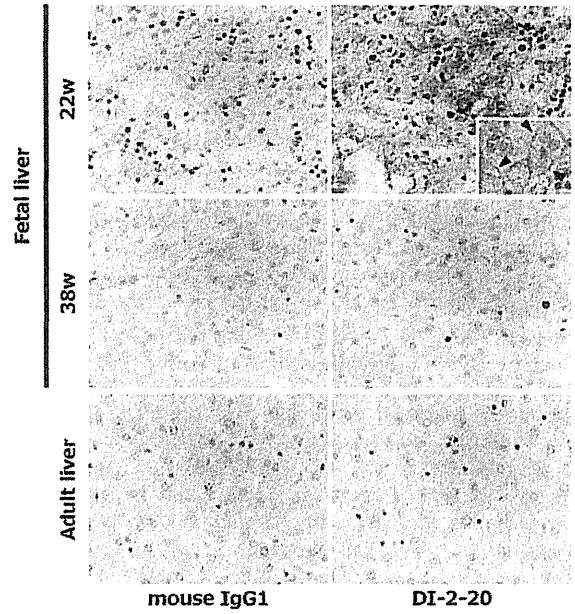

Fig. 2 Immunohistochemical analysis of hDlk-1 in foetal and adult liver. Each specimen was stained with anti-hDlk-1 mAb DI-2-20 (right panels). Foetal liver tissue at 22w (upper) shows membrane (arrow heads) and cytoplasmic staining with DI-2-20 monoclonal antibody. hDlk-1 staining was not observed in foetal liver at 38w (middle) and adult liver (lower). Mouse IgG1 used as isotype control was negative (left panels). Magnification is ×400.

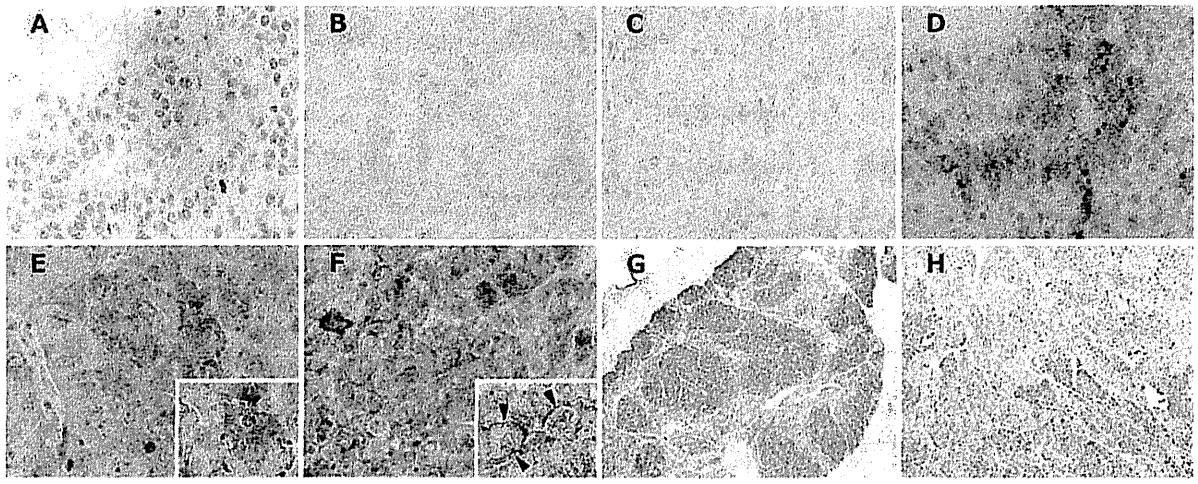

Fig. 3 hDlk-1 expression was observed only in hepatocellular carcinoma. Immunohistochemical staining with anti-hDlk-1 monoclonal antibody DI-2-20 was performed using tissue microarrays of liver tumour (388 malignant and 19 benign), nodular cirrhosis (40), viral hepatitis (11) and normal liver (26). The expression of hDlk-1 was detected only in HCC sections (D–F), not in adult liver (not shown), viral hepatitis (B), nodular cirrhosis (C), cavernous hemangioma (not shown) and intrahepatic cholangioma (not shown). hDlk-1 immunoreactivity in HCC cells was localized in either cytoplasm (E, inset) or cell membrane (F, inset). Membranous staining of hDlk-1 was shown by arrow heads. hDlk-1 expression was also examined in some samples of conventional tissue section corresponding to hDlk-1 positive spots in tissue array (G and H). Mouse IgG1 was used as negative control (A). Magnification is ×400 (A–F), ×1000 (inset in E and F) and ×40 (G and H).

cells. Additionally, hDlk-1 was also expressed in the cell surface of SK-N-F1 cells, a neuroblastoma cell line (Fig. 1C).

To evaluate the expression of hDlk-1 in non-neoplastic and neoplastic liver lesions, immunohistochemical analysis was performed by using tissue arrays. Typical staining profiles are shown in Fig. 3 and the results are summarized in Table I. hDlk-1 expression was undetectable at all in normal adult liver (0/26, not shown), non-neoplastic liver lesions, viral hepatitis (0/11, Fig. 3B) and nodular cirrhosis (0/40, Fig. 3C). hDlk-1 was also not found in cavernous hemangioma (0/19, not shown) and intrahepatic cholangioma (0/2, not shown). In contrast, hDlk-1 expression examined by DI-2-20 antibody was specifically observed in HCC and was positive for 79 out of 386 cases (20.5%, Fig. 3D–F). The pattern of hDlk-1 staining varied among individual tumours, e.g. hDlk-1 signal exhibited a uniform distribution within the tumour in one case (Fig. 3E, F), whereas it showed mosaic-like pattern in another case (Fig. 3D). Similar results were obtained with the same tissue array by using DI-6 antibody that recognizes a different epitope from DI-2-20 (not shown). Although hDlk-1 is a type I transmembrane protein, the immunoreactivity in HCC cells was mainly observed in the cytoplasm (Fig. 3E, inset), whereas hDlk-1 was expressed in cell surface in some cases (Fig. 3F, inset). We also examined some of conventional tissue slides corresponding to hDlk-1 positive spots in tissue arrays for hDlk-1 expression. The staining of hDlk-1 was not uniform, but covered more than 10% of the tumour in all tissue sections that we studied (Fig. 3G and H). No immunoreactivity was observed in normal tissues adjacent to the tumour (not shown).

Table I. Summary of immunohistochemical analysis.

	hDlk-1 staining	
	−	+
(A) *hDlk-1 expression in HCC (386 cases)*		
CS03-01-002 (Cybrdi)	40	15
CC03-01-001 (Cybrdi)	43	12
CC03-01-003 (Cybrdi)	46	10
CC03-02-001 (Cybrdi)	14	3
A204 (ISU ABXIS)	29	6
A204(II) (ISU ABXIS)	29	6
BC03013 (Biomax US)	49	10
OD-CT-DgLiv02-002 (Outdo bio.)	25	7
CS3 (HCC only) (Super Biochips)	32	10
Total	307 (79.5%)	79 (20.5%)
(B) *hDlk-1 expression in normal liver, non-neoplastic liver lesions, benign liver tumour and cholangiocarcinoma*		
Normal liver	23	0
Viral hepatitis	11	0
Nodular cirrhosis of liver	40	0
Cavernous hemangioma of liver	19	0
Intrahepatic cholangicarcinoma	2	0

As summarized in Table II, there was no clear correlation between hDlk-1 expression and pathological grade, gender, or aetiology such as HBV or HCV infection ($P > 0.05$ by χ^2 test). In contrast, hDlk-1 expression was clearly correlated with age or expression of alpha-fetoprotein (AFP). Interestingly, hDlk-1 expression was detected at higher frequency in HCC under 50 years old (51 out of 162 specimens, 31.5%), whereas the hDlk-1 positive HCC was dramatically decreased over 50 years old (28 out of 220 specimens, 12.7%). Especially, the hDlk-1 positive HCC was 43.1% (22 out of 51 specimens) under 40 years old. AFP is a well-established marker for HCC and was

Table II. Relationship of hDlk-1 expression and clinical features.

	hDlk-1			
	−	+	hDlk-1+ ratio	
Grade				
I	46	9	16.40%	
II	158	54	25.50%	
III	50	14	21.90%	$P=0.347$
Gender				
Male	245	59	19.40%	
Female	58	20	25.60%	$P=0.225$
Age				
40>	29	22	43.10%	
40–49	82	29	26.10%	
50–60	99	17	14.70%	
>60	93	11	10.60%	$P<0.01$
AFP				
−	179	25	12.30%	
+	26	25	49.00%	$P<0.01$
Aetiology				
HBV+	44	12	21.40%	
HCV+	6	0	0.00%	
−	7	1	12.50%	$P=0.393$

present in 51 of 255 cases (20.0%). hDlk-1 was detected in 25 of 51 AFP-positive HCCs (49.0%), whereas 25 of 204 AFP-negative HCCs (12.3%) were positive for hDlk-1. These results indicated that the hDlk-1 was expressed more frequently in a patient under 50 years old and in AFP-positive HCC.

Expression of hDlk-1 in other carcinomas

We then examined the expression of hDlk-1 in various carcinomas and found that hDlk-1 was highly and frequently expressed in colon adenocarcinoma (58.6%), breast carcinoma (39.0%), pancreatic carcinoma (30.8%) and lung carcinoma (30.2%), but not in ovarian carcinoma (13.2%) and gastric carcinoma (3.33%). Interestingly, in pancreatic carcinomas, hDlk-1+ cells were found more frequently in islet carcinoma (50.0%) than duct carcinoma (28.3%). In the lung carcinoma, hDlk-1 was expressed in small cell lung carcinoma (52.5%), but only few non-small cell carcinoma (8.9%) expressed hDlk-1 (Fig. 4, summarized in Table III). These results suggested that hDlk-1 was expressed in various carcinomas.

As described above, hDlk-1 was more frequently expressed in AFP-positive HCC. Therefore we examined the expression of hDlk-1 in other AFP positive cancer, AFP-producing gastric cancer. hDlk-1 was rarely expressed in gastric carcinoma (3.33%), but was positive for two out of 10 cases in AFP-producing gastric cancer (20.0%, Fig. 4G and H, summarized in Table III). Previously, Dezso *et al.* (*42*) reported that hDlk-1 was highly expressed in hepatoblastoma, AFP-positive liver cancer occurring in childhood. Together with our result, it was suggested that hDlk-1 was frequently expressed in AFP-positive cancers.

Discussion

Previously, we demonstrated that Dlk-1 is strongly expressed in hepatoblasts in mouse foetal liver, down-regulated in late gestation, and completely disappeared in neonatal and adult liver. Single Dlk-1+ cell isolated from ED14.5 liver exhibited high proliferating activity and was able to differentiate into both hepatocyte and biliary epithelial cell lineages (*10*). These findings suggested that Dlk-1 is a cell surface antigen of foetal hepatic stem/progenitor cells in the mouse. In this study we prepared mAbs against hDlk-1 and showed that the expression pattern of hDlk-1 is similar to mouse Dlk-1/Pref-1 during liver development, i.e. hDlk-1 is expressed in foetal liver but not in adult liver and hDlk-1 is present in both cell membrane and cytoplasm (Fig. 2). Thus, hDlk-1 may be an excellent marker of foetal hepatic stem/progenitor cells in human as well.

In adult liver, hepatic progenitor cells (HPCs) appear around the portal vein when liver is severely injured. These cells are known as hepatic oval cells in rodents and express markers of both hepatocytes and biliary epithelium (*29*). HPCs in chronic liver diseases are suggested to contribute to liver regeneration as well as hepatocarcinogenesis (*43–45*). Dlk-1 is not expressed in normal liver and was found in a subpopulation of hepatic oval cells induced in rats treated with 2-acetylaminofluorene and partial hepatectomy, a well-established rat model of hepatic oval cell induction (*31*). However, in a mouse model of hepatic oval cell induction by 3,5-diethoxycarbonyl-1,4-dihydrocollidine (DDC) diet, Dlk-1 is not expressed in hepatic oval cells (*46*). In the present study, hDlk-1 immunoreactive cells were not found in the specimens of viral hepatitis and nodular cirrhosis. In contrast, it was expressed frequently in HCC, but not in intrahepatic cholangioma, cavernous hemangioma and non-neoplastic liver lesions. These results demonstrate that hDlk-1 is expressed in HCC at high frequency, but do not exclude the possibility that Dlk-1 is expressed in some of adult hepatic stem/progenitor cells in chronically injured liver, which can lead to tumourigenesis.

It still remains unclear whether liver tumour is derived from hepatic stem/progenitor cells or mature hepatocytes. Recently, Lee *et al.* (*47*) reported that two subtypes (HB and HC) of HCC were categorized by analysis of gene expression patterns, and suggested that they may reflect the origin of tumour cells. The HB subtype shared a gene expression pattern with foetal hepatoblasts, whereas the HC subtype shared with adult hepatocytes, suggesting that the HB subtype may arise from hepatic stem/progenitor cells. The HB subtype of HCC showed poor prognosis compared to HC subtype. Interestingly, the HB subtype accounts for ~20% of HCC examined, similar to the frequency of hDlk-1 positive cells. In addition, the expression of hDlk-1 was more frequently found in HCC patients younger than 50 years old. Because HCC develops after a long latency period of chronic infection with HBV, HCV or both, the incidence of HCC is relatively high over 50 years old. Therefore, our finding that HCC patients under 50 years old expressed hDlk-1

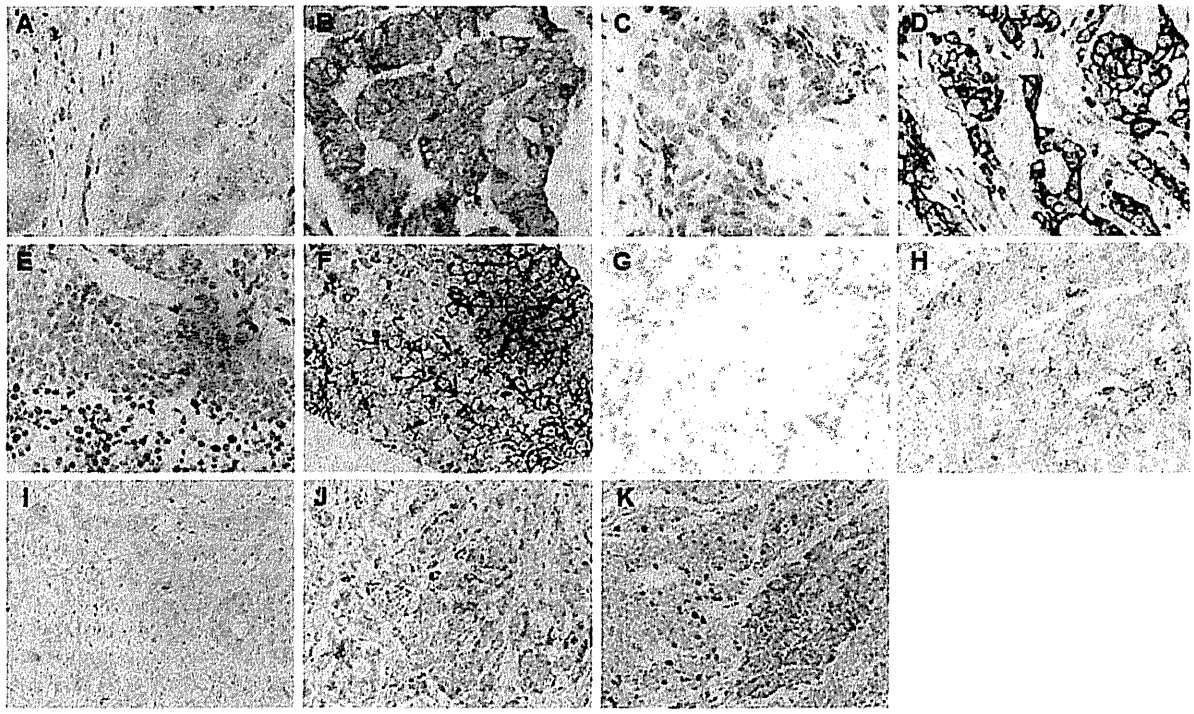

Fig. 4 hDlk-1 expression in various tumours. hDlk-1 expression in various tumours were examined by immunohistochemistry using anti-hDlk-1 mAb, DI-2-20. (A and B) Colon adenocarcinoma, (C and D) breast carcinoma, (E and F) small cell lung carcinoma, (G and H) AFP-producing gastric cancer, (I and J) pancreatic adenocarcinoma, (K) islet cell carcinoma. Tumour cells showed strong staining in cytoplasm (J and K), and cytoplasm and cell membrane (B, D, F and H). A, C, E, G and I showed hDlk-1 negative tumour cells. Magnification is ×200.

Table III. Summary of hDlk-1 staining in various tumours.

Tumour		Dlk−	Dlk+	Total
Colon adenocarcinoma		24 (41.4%)	34 (58.6%)	58
Ovarian carcinoma		59 (86.8%)	9 (13.2%)	68
Pancreatic carcinoma	Duct adenocarcinoma	33 (71.7%)	13 (28.3%)	46
	Islet cell carcinoma	3 (50.0%)	3 (50.0%)	6
Breast carcinoma		36 (61.0%)	23 (39.0%)	59
Lung carcinoma	NSCLC	51 (91.1%)	5 (8.9%)	56
	SCLC	19 (47.5%)	21 (52.5%)	30
Gastric carcinoma		29 (96.7%)	1 (3.33%)	30
AFP-producing gastric cancer	8 (80%)	2 (20%)	10	

more frequently is unexpected and intriguing. However, there was so far no clear correlation between hDlk-1 positive tumours in patients under 50 years old and specific aetiologies such as gender, pathological grade and stage. Recently, Huang *et al.* (*48*) also reported that hDlk-1 expression in HCC showed no significant correlation with HBV infection, tumour size and serology of AFP. Thus, our finding suggests that hDlk-1+ HCC develops in a relatively short latency period and may have an origin different from other HCC with a longer latency period. Alternatively, considering the recent finding that albumin positive hepatocytes can be converted into induced pluripotent stem cells (iPS) by transient expression of c-Myc, Sox2, Oct3/4 and Klf4 (*49*), conversion of mature hepatocytes to an immature stage with hDlk-1 expression may occur during chronic liver injury. Thus, it is tempting to speculate that hDlk-1 may be a hallmark of HCC originated from hepatic or cancer stem/progenitor cells. The origin and mechanism of tumourigenesis of HCC still need extensive investigation.

While Dlk-1, also known as Pref-1, was originally described as an inhibitor of adipogenesis (*8*), the precise function still remains unknown. In this study, we showed that hDlk-1 is expressed in not only HCC but also many carcinomas such as colon, breast, pancreatic and lung carcinomas. As previously reported, colony formation, cell growth and tumourigenicity of HCC cell lines were significantly decreased when the endogenous hDlk-1 was knocked down by RNAi (*48*), and hDlk-1 promoted proliferation of glioblastoma cell line (GBM cells) (*24*) and erythroid leukemia cell line (K562 cells) (*26*). Furthermore, Dlk-1 has been reported to interact with Notch 1, and modulate

Notch signalling as a negative regulator (*50*). Notch 1 signalling prevented HCC cells to proliferate by induction of cell cycle arrest and apoptosis (*51*). Thus, hDlk-1 may contribute to tumourigenesis by enhancing tumour growth. However, precise molecular mechanism of Dlk functions is still unknown, and requires further studies. Because hDlk-1 is a cell surface molecule expressed in many HCCs and also other carcinomas, but neither in normal adult liver nor most of the tissues, it may be an attractive target for antibody therapy. In this study, we established many monoclonal antibodies against hDlk-1, and now we are developing monoclonal antibodies against hDlk-1 that block proliferation of HCC in a xenograft model.

Conflict of interest
None declared.

References

1. Parkin, D.M., Bray, F., Ferlay, J., and Pisani, P. (2001) Estimating the world cancer burden: Globocan 2000. *Int. J. Cancer* **94**, 153–156
2. El-Serag, H.B. and Mason, A.C. (1999) Rising incidence of hepatocellular carcinoma in the United States. *New Engl. J. Med.* **340**, 745–750
3. Okuda, K. (2000) Hepatocellular carcinoma. *J. Hepatol* **32**, 225–237
4. Halder, S.K., Takemori, H., Hatano, O., Nonaka, Y., Wada, A., and Okamoto, M. (1998) Cloning of a membrane-spanning protein with epidermal growth factor-like repeat motifs from adrenal glomerulosa cells. *Endocrinology* **139**, 3316–3328
5. Jensen, C.H., Krogh, T.N., Højrup, P., Clausen, P.P., Skjødt, K., Larsson, L.I., Enghild, J.J., and Teisner, B. (1994) Protein structure of fetal antigen 1 (FA1). A novel circulating human epidermal-growth-factor-like protein expressed in neuroendocrine tumors and its relation to the gene products of dlk and pG2. *Eur. J. Biochem.* **225**, 83–92
6. Laborda, J., Sausville, E.A., Hoffman, T., and Notario, V. (1993) dlk, a putative mammalian homeotic gene differentially expressed in small cell lung carcinoma and neuroendocrine tumor cell line. *J. Biol. Chem.* **268**, 3817–3820
7. Lee, Y.L., Helman, L., Hoffman, T., and Laborda, J. (1995) dlk, pG2 and Pref-1 mRNAs encode similar proteins belonging to the EGF-like superfamily. Identification of polymorphic variants of this RNA. *Biochim. Biophys. Acta* **1261**, 223–232
8. Smas, C.M. and Sul, H.S. (1993) Pref-1, a protein containing EGF-like repeats, inhibits adipocyte differentiation. *Cell* **73**, 725–734
9. Floridon, C., Jensen, C.H., Thorsen, P., Nielsen, O., Sunde, L., Westergaard, J.G., Thomsen, S.G., and Teisner, B. (2000) Does fetal antigen 1 (FA1) identify cells with regenerative, endocrine and neuroendocrine potentials? A study of FA1 in embryonic, fetal, and placental tissue and in maternal circulation. *Differentiation* **66**, 49–59
10. Tanimizu, N., Nishikawa, M., Saito, H., Tsujimura, T., and Miyajima, A. (2003) Isolation of hepatoblasts based on the expression of Dlk/Pref-1. *J. Cell Sci.* **116**, 1775–1786
11. Schmidt, J.V., Matteson, P.G., Jones, B.K., Guan, X.J., and Tilghman, S.M. (2000) The Dlk1 and Gtl2 genes are linked and reciprocally imprinted. *Genes Dev.* **14**, 1997–2002
12. Laborda, J. (2000) The role of the epidermal growth factor-like protein dlk in cell differentiation. *Histol. Histopathol.* **15**, 119–129
13. Beatus, P. and Lendahl, U. (1999) Notch and neurogenesis. *J. Neurosci. Res.* **54**, 125–136
14. Artavanis-Tsakonas, S., Rand, M.D., and Lake, R.J. (1999) Notch signaling: cell fate control and signal integration in development. *Science* **284**, 770–776
15. Smas, C.M. and Sul, H.S. (1996) Characterization of Pref-1 and its inhibitory role in adipocyte differentiation. *Int. J. Obes. Relat. Metab. Disord.* **20 (Suppl. 3)**, S65–S72
16. Jordan, C.T. and Van Zant, G. (1998) Recent progress in identifying genes regulating hematopoietic stem cell function and fate. *Curr. Opin. Cell Biol.* **10**, 716–720
17. Moore, K.A., Pytowski, B., Witte, L., Hicklin, D., and Lemischka, I.R. (1997) Hematopoietic activity of a stromal cell transmembrane protein containing epidermal growth factor-like repeat motifs. *Proc. Natl. Acad. Sci. USA* **94**, 4011–4016
18. Tornehave, D., Jansen, P., Teisner, B., Rasmussen, H.B., Chemnitz, J., and Moscoso, G. (1993) Fetal antigen 1 (FA1) in the human pancreas: cell type expression, topological and quantitative variations during development. *Anat. Embryol. (Berl.)* **187**, 335–341
19. Tornehave, D., Jensen, C.H., Teisner, B., and Larsson, L.I. (1996) FA1 immunoreactivity in endocrine tumours and during development of the human fetal pancreas; negative correlation with glucagon expression. *Histochem. Cell Biol.* **106**, 535–542
20. Jensen, C.H., Teisner, B., Højrup, P., Rasmussen, H.B., Madsen, O.D., Nielsen, B., and Skjødt, K. (1993) Studies on the isolation, structural analysis and tissue localization of fetal antigen 1 and its relation to a human adrenal-specific cDNA, pG2. *Hum. Reprod.* **8**, 635–641
21. Cooper, M.J., Hutchins, G.M., Cohen, P.S., Helman, L.J., Mennie, R.J., and Israel, M.A. (1990) Human neuroblastoma tumor cell lines correspond to the arrested differentiation of chromaffin adrenal medullary neuroblasts. *Cell Growth Differ.* **1**, 149–159
22. Gaetano, C., Matsumoto, K., and Thiele, C.J. (1992) In vitro activation of distinct molecular and cellular phenotypes after induction of differentiation in a human neuroblastoma cell line. *Cancer Res.* **52**, 4402–4407
23. Hsiao, C.C., Huang, C.C., Sheen, J.M., Tai, M.H., Chen, C.M., Huang, L.L., and Chuang, J.H. (2005) Differential expression of delta-like gene and protein in neuroblastoma, ganglioneuroblastoma and ganglioneuroma. *Mod. Pathol.* **18**, 656–662
24. Yin, D., Xie, D., Sakajiri, S., Miller, C.W., Zhu, H., Popoviciu, M.L., Said, J.W., Black, K.L., and Koeffler, H.P. (2006) DLK1: increased expression in gliomas and associated with oncogenic activities. *Oncogene* **25**, 1852–1861
25. Harken Jensen, C., Drivsholm, L., Laursen, I., and Teisner, B. (1999) Elevated serum levels of fetal antigen 1, a member of the epidermal growth factor superfamily, in patients with small cell lung cancer. *Tumour Biol.* **20**, 256–262
26. Sakajiri, S., O'kelly, J., Yin, D., Miller, C.W., Hofmann, W.K., Oshimi, K., Shih, L.Y., Kim, K.H., Sul, H.S., Jensen, C.H., Teisner, B., Kawamata, N., and Koeffler, H.P. (2005) Dlk1 in normal and abnormal hematopoiesis. *Leukemia* **19**, 1404–1410
27. Altenberger, T., Bilban, M., Auer, M., Knosp, E., Wolfsberger, S., Gartner, W., Mineva, I., Zielinski, C., Wagner, L., and Luger, A. (2006) Identification of DLK1

variants in pituitary- and neuroendocrine tumors. *Biochem. Biophys. Res. Commun.* **340**, 995–1005
28. Fukuzawa, R., Heathcott, R.W., Morison, I.M., and Reeve, A.E. (2005) Imprinting, expression, and localisation of DLK1 in Wilms tumours. *J. Clin. Pathol.* **58**, 145–150
29. Fausto, N. and Campbell, J.S. (2003) The role of hepatocytes and oval cells in liver regeneration and repopulation. *Mech. Dev.* **120**, 117–130
30. Shupe, T. and Petersen, B.E. (2005) Evidence regarding a stem cell origin of hepatocellular carcinoma. *Stem Cell Rev.* **1**, 261–264
31. Tanimizu, N., Tsujimura, T., Takahide, K., Kodama, T., Nakamura, K., and Miyajima, A. (2004) Expression of Dlk/Pref-1 defines a subpopulation in the oval cell compartment of rat liver. *Gene Expr. Patterns* **5**, 209–218
32. Singh, S.K., Clarke, I.D., Hide, T., and Dirks, P.B. (2004) Cancer stem cells in nervous system tumors. *Oncogene* **23**, 7267–7273
33. Al-Hajj, M., Becker, M.W., Wicha, M., Weissman, I., and Clarke, M.F. (2004) Therapeutic implications of cancer stem cells. *Curr. Opin. Genet. Dev.* **14**, 43–47
34. Reya, T., Morrison, S.J., Clarke, M.F., and Weissman, I.L. (2001) Stem cells, cancer, and cancer stem cells. *Nature* **414**, 105–111
35. Al-Hajj, M., Wicha, M.S., Benito-Hernandez, A., Morrison, S.J., and Clarke, M.F. (2003) Prospective identification of tumorigenic breast cancer cells. *Proc. Natl. Acad. Sci. USA* **100**, 3983–3988
36. Al-Hajj, M. and Clarke, M.F. (2004) Self-renewal and solid tumor stem cells. *Oncogene* **23**, 7274–7282
37. Olempska, M., Eisenach, P.A., Ammerpohl, O., Ungefroren, H., Fandrich, F., and Kalthoff, H. (2007) Detection of tumor stem cell markers in pancreatic carcinoma cell lines. *Hepatobiliary Pancreat. Dis. Int.* **6**, 92–97
38. O'Brien, C.A., Pollett, A., Gallinger, S., and Dick, J.E. (2007) A human colon cancer cell capable of initiating tumour growth in immunodeficient mice. *Nature* **445**, 106–110
39. Singh, S.K., Hawkins, C., Clarke, I.D., Squire, J.A., Bayani, J., Hide, T., Henkelman, R.M., Cusimano, M.D., and Dirks, P.B. (2004) Identification of human brain tumour initiating cells. *Nature* **432**, 396–401
40. Collins, A.T., Berry, P.A., Hyde, C., Stower, M.J., and Maitland, N.J. (2005) Prospective identification of tumorigenic prostate cancer stem cells. *Cancer Res.* **65**, 10946–10951
41. Ma, S., Chan, K.W., Hu, L., Lee, T.K., Wo, J.Y., Ng, I.O., Zheng, B.J., and Guan, X.Y. (2007) Identification and characterization of tumorigenic liver cancer stem/progenitor cells. *Gastroenterology* **132**, 2542–2556
42. Dezso, K., Halász, J., Bisgaard, H.C., Paku, S., Turányi, E., Schaff, Z., and Nagy, P. (2008) Delta-like protein (DLK) is a novel immunohistochemical marker for human hepatoblastomas. *Virchows Arch.* **452**, 443–448
43. Libbrecht, L. and Roskams, T. (2002) Hepatic progenitor cells in human liver diseases. *Semin. Cell Dev. Biol.* **13**, 389–396
44. Lowes, K.N., Brennan, B.A., Yeoh, G.C., and Olynyk, J.K. (1999) Oval cell numbers in human chronic liver diseases are directly related to disease severity. *Am. J. Pathol.* **154**, 537–541
45. Eleazar, J.A., Memeo, L., Jhang, J.S., Mansukhani, M.M., Chin, S., Park, S.M., Lefkowitch, J.H., and Bhagat, G. (2004) Progenitor cell expansion: an important source of hepatocyte regeneration in chronic hepatitis. *J. Hepatol.* **41**, 983–991
46. Jelnes, P., Santoni-Rugiu, E., Rasmussen, M., Friis, S.L., Nielsen, J.H., Tygstrup, N., and Bisgaard, H.C. (2007) Remarkable heterogeneity displayed by oval cells in rat and mouse models of stem cell-mediated liver regeneration. *Hepatology* **45**, 1462–1470
47. Lee, J.S., Heo, J., Libbrecht, L., Chu, I.S., Kaposi-Novak, P., Calvisi, D.F., Mikaelyan, A., Roberts, L.R., Demetris, A.J., Sun, Z., Nevens, F., Roskams, T., and Thorgeirsson, S.S. (2006) A novel prognostic subtype of human hepatocellular carcinoma derived from hepatic progenitor cells. *Nat. Med.* **12**, 410–416
48. Huang, J., Zhang, X., Zhang, M., Zhu, J.D., Zhang, Y.L., Lin, Y., Wang, K.S., Qi, X.F., Zhang, Q., Liu, G.Z., Yu, J., Cui, Y., Yang, P.Y., Wang, Z.Q., and Han, Z.G. (2007) Up-regulation of DLK1 as an imprinted gene could contribute to human hepatocellular carcinoma. *Carcinogenesis* **28**, 1094–1103
49. Takahashi, K., Tanabe, K., Ohnuki, M., Narita, M., Ichisaka, T., Tomoda, K., and Yamanaka, S. (2007) Induction of pluripotent stem cells from adult human fibroblasts by defined factors. *Cell* **131**, 861–872
50. Baladrón, V., Ruiz-Hidalgo, M.J., Nueda, M.L., Díaz-Guerra, M.J., García-Ramírez, J.J., Bonvini, E., Gubina, E., and Laborda, J. (2005) dlk acts as a negative regulator of Notch 1 activation through interactions with specific EGF-like repeats. *Exp. Cell Res.* **303**, 343–359
51. Qi, R., An, H., Yu, Y., Zhang, M., Liu, S., Xu, H., Guo, Z., Cheng, T., and Cao, X. (2003) Notch 1 signaling inhibits growth on human hepatocellular carcinoma through induction of cell cycle arrest and apoptosis. *Cancer Res.* **63**, 8323–8329

Pathology International

Pathology International 2010; **60**: 575–580 doi:10.1111/j.1440-1827.2010.02565.x

Original Article

Cytokeratin expression profiling is useful for distinguishing between primary squamous cell carcinoma of the lung and pulmonary metastases from tongue cancer

Takehiko Ohba,[1,2] Noriko Motoi,[1] Yukinori Kimura,[1] Sakae Okumura,[3] Kazuyoshi Kawabata,[4] Yasuyuki Yoshizawa,[2] Naohiko Inase[2] and Yuichi Ishikawa[1]

[1]Division of Pathology, The Cancer Institute, Departments of [3]Thoracic Surgical Oncology and [4]Head and Neck Oncology, The Cancer Institute Hospital, Japanese Foundation for Cancer Research and [2]Department of Integrated Pulmonology, Tokyo Medical and Dental University, Tokyo, Japan

It can be difficult to distinguish between primary and metastatic squamous cell carcinoma (SCC) in the lung. Surgical specimens were obtained from two groups of patients, 26 lung SCC patients without histories of any other cancer (the definite primary group) and 17 patients who had undergone surgical removal of SCC emerging in the lung after surgery for tongue SCC (the unknown group). From the former, 26 primary lung SCC were obtained. From the latter, 17 lung tumors and 15 primary tumors of the tongue were obtained. Eleven of the 17 lung tumors from the unknown group were metastatic lung SCC. All specimens were immunostained with cytokeratin (CK)5/6, CK7, CAM5.2, CK19 and p63 antibodies. The frequency of CAM5.2 and CK19 expression was significantly higher in the lung SCC of the definite primary group (21 of 26, 81% and 20 of 26, 78%, respectively) than in the metastatic lung SCC (1 of 11, 9% ($P < 0.001$) and 2 of 11, 18% ($P = 0.003$), respectively) or primary SCC of the tongue (5 of 15, 33% ($P = 0.002$) and 2 of 15, 13% ($P < 0.001$), respectively). CAM5.2 and CK19 are useful for distinguishing between primary SCC of the lung and metastases from tongue cancer.

Key words: cytokeratin, lung cancer, metastasis, squamous cell carcinoma, tongue cancer

The lung is a common site of primary tumors as well as metastatic lesions. Primary lung adenocarcinomas have features that are morphologically and immunohistochemically distinct from those of other organs such as colorectal adenocarcinomas. Therefore, it is not difficult to differentiate between primary lung adenocarcinomas and metastatic tumors from other sites. However, squamous cell carcinomas (SCC) pose a greater challenge. When a patient with a history of tongue SCC develops an SCC in the lung, it can be difficult to determine whether the new tumor is a primary lung cancer or a metastasis from the tongue. This distinction is clinically important for several reasons: SCC of the tongue sometimes recurs as a distant metastasis (4.8–8.0%),[1,2] often in the lung;[3] SCC is one of the major histological subtypes of primary lung cancer; and therapeutic strategies and prognoses are quite different between cases with primary and metastatic tumors. Similarities in the etiologies and histological features of these tumors contribute to the difficulty in determining the tumor's origin.

Cytokeratin (CK) polypeptides are the major cytoskeletal proteins in epithelial cells. CK has been separated by molecular weights into at least twenty subtypes, which are expressed in various combinations depending on the epithelial cell type. Roughly speaking, relatively high molecular weight CK is characteristic of squamous epithelium, whereas lower molecular weight CK typifies simple columnar epithelium.[4,5] SCC arising from tissues with true squamous epithelium usually express CK characteristics of squamous epithelium. On the other hand, primary lung SCC express CK characteristics of columnar epithelium, such as CK8, 18 and 19, more abundantly than do SCC of tissues with true squamous epithelium, including the oral cavity, esophagus, vulva and skin.[6] CK19 is also expressed more frequently and intensely in lung SCC than in oral SCC.[7] These reports suggest that primary lung SCC arising from columnar epithelium through a metaplastic process may have a somewhat different CK profile from those arising from true squamous

Correspondence: Yuichi Ishikawa, MD, PhD, Division of Pathology, The Cancer Institute, Japanese Foundation for Cancer Research, 3-8-31 Ariake, Koto-ku, Tokyo 135-8550, Japan. Email: ishikawa@jfcr.or.jp

Received 11 January 2010. Accepted 24 April 2010.

epithelium. However, to the best of our knowledge, there are no reports on whether CK expression patterns can be used to distinguish between primary lung SCC and metastatic lung SCC from another organ. We determined that primary lung SCC can be differentiated from metastatic lung SCC of the tongue by analyzing their CK expression pattern.

METHODS

Patients and materials

Between 1977 and 2008, 17 patients with histories of surgical treatment for tongue SCC underwent surgery for lung SCC at our hospital. Since it was unknown whether each of these lung tumors was a primary tumor or a metastasis from the tongue, we termed these patients the 'unknown group'. Seventeen lung SCC and 15 primary tongue SCC tumors (specimens of two cases were not available) were obtained from the unknown group. Additionally, 26 patients who underwent surgery for primary lung SCC at the same hospital in 1998 without a history of any other cancer were selected randomly for comparison. Since the tumors of the latter group were definitely primary lung cancers, we termed these patients the 'definite primary group.' Tumor specimens were obtained from all 26 patients in this group. This study was performed with informed consent and followed the guidelines for experimental investigation with human subjects required by the institution.

At first, we classified the lung tumors of the unknown group (Cases 1–17) into three subgroups, metastatic, primary or unclassified. Traditionally, these diagnoses are based on clinicopathological findings, such as tumor location, number of lesions or pathological comparisons with the putative primary tumor. But this approach does not always give a definite diagnosis. Therefore, we made the diagnoses considering prognosis after lung surgery as well. The criteria used in this study are shown in Table 1. Fifteen cases were classified as metastases or primaries in a mutually exclusive manner. The other two cases remained unclassified by these criteria. The diagnostic procedures are summarized in Table 2. Cases 8–11 satisfied only one metastasis criterion. In fact, Cases 8–10 died within one year of resection of their lung tumors, which was relatively soon for surgical cases of primary lung SCC. Case 11 was 23 years old at the time the lung tumor developed, which was very young for primary lung SCC. None of Cases 8-11 satisfied any of the five primary items. Thus, they were considered metastases of tongue SCC. The lung tumor of Case 14 had extensive *in situ* spreading. The lung tumor of Case 15 was centrally located. Additionally, neither Case 14 nor Case 15 satisfied any criteria characteristic of a metastasis. Thus, they were considered likely primary lung tumors. Case 16 and Case 17 showed both primary and metastatic characteristics, and so they remained unclassified. In total, 11 lung tumors from the unknown group were diagnosed as metastatic lung SCC.

Table 1 Diagnostic criteria for squamous cell carcinoma (SCC) observed in the unknown group

Pro metastasis findings
(1) Multiple lung lesions of similar size were present.
(2) Survival time after removal of the lung tumor was less than 6 months.
(3) Histological features favored a metastasis (i.e. similar cellular appearance in both lung and tongue SCC or exceeding central necrosis in the lung tumor).
Pro primary findings
(4) Pathological N0 of the tongue SCC was proved.
(5) *In situ* carcinoma was seen in the lung tumor.
(6) The tongue SCC had been controlled for more than 2 years before the emergence of a lung tumor.
(7) Survival time after removal of the lung tumor was more than 3 years.
(8) The site of the lung lesion was central (i.e. in the main, lobular or segmental bronchus).

N0, no metastasis to lymphnodes.

Table 2 Final tumor classification results (metastatic, primary or unclassified) for the unknown group

	Satisfied diagnostic criteria†		
Case	pro metastasis	pro primary	Diagnosis
1	(1), (3)	None	Metastasis
2	(1), (2), (3)	None	Metastasis
3	(2), (3)	None	Metastasis
4	(2), (3)	None	Metastasis
5	(2), (3)	None	Metastasis
6	(2), (3)	None	Metastasis
7	(2), (3)	None	Metastasis
8	(3)	None	Metastasis
9	(3)	None	Metastasis
10	(3)	None	Metastasis
11	(3)	None	Metastasis
12	None	(5), (6), (7), (8)	Primary
13	None	(4), (5)	Primary
14	None	(5)	Primary
15	None	(8)	Primary
16	(3)	(7)	Unclassified
17	(1)	(4)	Unclassified

†See Table 1 for definitions of the diagnostic criteria.

Immunohistochemistry

The specimens were prepared from formalin-fixed, paraffin-embedded tissue blocks. The primary antibodies used in this study are listed in Table 3. CK5/6 reacts with CK5 and CK6, which are high molecular weight keratins that are expressed in squamous epithelium. CK7 and CK19 are relatively low molecular weight CK expressed in columnar epithelium, and they are not normally expressed in stratified squamous epithelium. CAM5.2, which has primary reactivity with CK8 and weaker but distinct reactivity with CK7, reacts with most

Table 3 Antibodies for cytokeratins used in this study

Antibody	Source	Clone	Dilution	HIER
CK5/6	Chemicon Illinois, USA	D5/16B4	1:100	In citrate (pH 6.0)
CK7	Progen Heidelberg Germany	OVTL12-30	1:50	In Tris-EDTA (pH 9.0)
CAM5.2	Becton-Dickinson San Jose, CA, USA	CAM5.2	prediluted	In Tris-EDTA (pH 9.0)
CK19	Dako Glostrup, Denmark	RCK108	1:20	In citrate (pH 6.0)
p63	Thermo-Scientific Fermont, CA, USA	4A4	1:100	In citrate (pH 6.0)

HIER, heat-induced epitope retrieval.

Table 4 Clinicopathological characteristics of examined patients with definite primary or unknown lung squamous cell carcinomas. For final diagnosis of the unknown group, see Table 2 and text

Group	Definite primary		Unknown	
Final diagnosis	Primary ($n = 26$)	Metastasis ($n = 11$)	Primary ($n = 4$)	Unclassified ($n = 2$)
Age				
Mean (years)	69.0	46.3*	61.8	46.0
Sex				
Male/Female	22/4	6/5	4/0	1/1
Smoking index†				
Mean	1287	396*	1298	630
Differentiation				
W/M+P	3/23	7/4*	2/2	0/2
Size of lung tumor				
Mean (mm)	50.2	38.6	47.3	23.5
Location of lung tumor				
Peripheral/Central	18/8	11/0	2/2	2/0
Stage of lung tumor				
I/II + III	13/13	2/9	2/2	1/1

*$P < 0.01$. P-values for comparisons between the definite primary group and the unknown group (P-values for age, smoking index and tumor size were obtained by Welch's t-test and those for sex, tumor site, differentiation and stage were obtained by chi-squared test).

†Smoking index, a product of the numbers of cigarette per day and duration (years).

W, well differentiated; M+P, moderately or poorly differentiated.

epithelial cells with the exception of stratified squamous epithelium.[8,9] p63, a nuclear transcription factor predominantly expressed in stratified epithelium,[10] was also evaluated. After deparaffinization, the sections were submerged in either sodium citrate buffer or Tris-EDTA buffer for heat-induced epitope retrieval at 97°C for 40 min. The immunostaining was carried out using the EnVision+ dextran polymer kit (Dako, Glostrup, Denmark) in Dako Autostainer (Dako, Glostrup, Denmark). Immunoreactivity was regarded as positive when 10% or more of tumor cells were stained.

Statistical analysis

Statistical analyses for correlation of clinicopathological features were performed by the chi-squared test and Welch's t-test. Statistical analyses for immunoreactivity were performed by the chi-squared test. Differences at $P < 0.05$ were regarded as significant.

RESULTS

Clinicopathological characteristics of patients examined

The patient characteristics are shown in Table 4. Compared with the definite primary group, cases of the unknown group whose lung tumors were diagnosed as metastases showed significantly younger onset, lower cumulative smoking and a higher proportion of well-differentiated tumors. On the other hand, primary tumors of the unknown group showed quite similar characteristics to the definite primary group: older age and high cumulative smoking history.

Immunohistochemical results

CK were localized to the cytoplasm and along the cell membrane. The staining of CK5/6 was strong and widely distributed both in tumor and in normal squamous cells. Staining of

Table 5 Positive ratio of each cytokeratin and p63 in the definite primary group and the unknown group

Group	Definite primary		Unknown		
Tumor site			Lung		
Diagnosis	Lung	Metastasis	Primary	Unclassified	Tongue
CK5/6	26/26	10/11	3/4	2/2	15/15
CK7	4/26	0/11	2/4	0/2	1/15
CAM5.2	21/26	1/11*	2/4	1/2	5/15*
CK19	20/26	2/11*	2/4	0/2	2/15*
p63	25/26	9/11	3/4	2/2	12/15

*$P < 0.01$. *P*-values for comparisons between the definite primary group and the unknown group (obtained by chi-squared test).

CK7, CAM5.2 and CK19 was observed in tumor cells as well as in normal bronchial epithelium, but not in normal squamous epithelium. In tumor cells, reactions were mainly observed in non-keratinized components. p63 staining was observed in the nuclei of tumor cells and normal squamous epithelial cells. Staining patterns of p63 were similar between primary tongue carcinomas and their metastases to the lung.

The frequency of the CK- and p63-positive tumors in each group is shown in Table 5. The expression of CAM5.2 in the lung SCC of the definite primary group (21 of 26, 81%) was significantly higher than in the primary SCC of the tongue (5 of 15, 33% ($P = 0.002$)) or the metastatic lung SCC (1 of 11, 9% ($P < 0.001$)). Also, the expression of CK19 in lung SCC of the definite primary group (20 of 26, 78%) was significantly higher than in the primary tumors of the tongue (2 of 15, 13% ($P < 0.001$)) or in the metastatic lung SCC (2 of 11, 18% ($P = 0.003$)). Representative images of tumors immunostained with CAM5.2 and CK19 are shown in Fig. 1. There are two types of primary SCC of the lung based on location, peripheral and central. However, we found no difference of reactivity of CAM5.2 and CK19 in the central and peripheral tumors. In fact, for CAM5.2 the positive frequency in central and peripheral types was 6 of 8 and 15 of 18, and for CK19 that was 6 of 8 and 14 of 18, respectively, which were not significantly different.

In all SCC CK5/6 and p63 were expressed very frequently and CK7 was rarely expressed. For distinguishing between primary tumors and metastases, the use of CAM5.2 and CK19 provided 81% and 78% sensitivity and 91% and 82% specificity, respectively. Both CAM5.2 and CK19 tended to be expressed more often in basal and parabasal tumor cells, which showed minimal squamous differentiation, than in upper layer cells or keratinizing cells. This was the case for both primary lung and tongue tumors and metastatic tumors. In other words, the two CK tended to be positive in basal or poorly-differentiated components, and to be negative in well-differentiated components.

Details of CAM5.2 and CK19 expression in the 11 metastatic tumors are listed in Table 6. The expression patterns were consistent in 90% (9/10) for CAM5.2 and 70% (7/10) for CK19, indicating relatively consistent expression patterns before and after metastasis.

DISCUSSION

When a lung SCC is detected in a patient with a history of tongue SCC, it may be difficult to make a distinction between a new primary tumor and a metastasis. Our results show that primary lung SCC express CAM5.2 and CK19 significantly more frequently than do metastatic lung SCC from the tongue, and CK are useful for differentiating between the tumor types. To the best of our knowledge, this is the first report to demonstrate the usefulness of CK expression patterns for distinguishing primary lung SCC from metastases.

To characterize CK profiles of metastatic lung SCC, we had to determine whether each of the lung tumors of the unknown group was primary or metastatic. We used the original criteria that include clinical course after lung surgery. Our criteria clearly identified 15 of 17 lung squamous tumors of the unknown group as primary or metastatic tumors. The patients who were diagnosed with metastases showed significantly younger ages of onset and lower cumulative smoking than the definite primary group. These characteristic features backed up our criteria, because tongue SCC patients are younger than those with primary lung SCC,[11–14] and because risk factors for tongue SCC include not only smoking but also alcohol intake, among other things.[12,15,16] Meanwhile, patients who were diagnosed with primary tumors showed similar characteristics to the definite primary group. These findings suggest that our criteria were largely appropriate. CAM5.2 and/or CK19 expression between primary and metastatic sites did not accord in three cases. The discrepancy may be due partly to heterogeneity of tumor cell characteristics. All tongue tumors in these three cases showed heterogeneous expression of CK. Specifically, two cases, judged as negative, included a small number of positively staining cells (<10%), and the other one, judged as positive, also had a negatively staining component (about 80%). Such components contradicting the final judgment might have metastasized to the lung.

CK, which are constituents of intermediate filaments of epithelial cells, are divided into at least twenty subtypes. The profile of CK expression differs depending on the epithelial cell type and the degree of cellular differentiation. We showed that primary lung SCC more frequently express

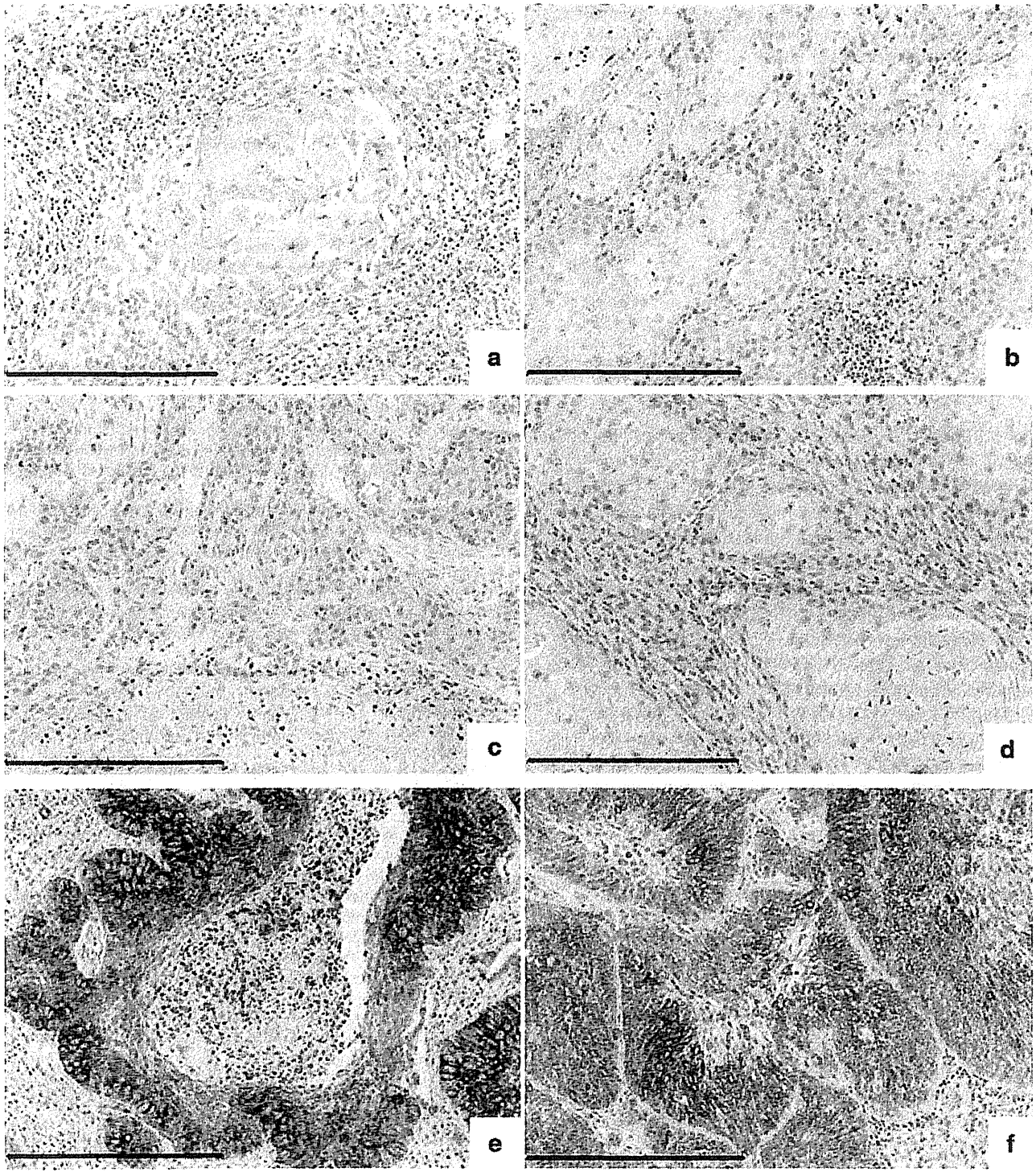

Figure 1 Representative images of squamous cell carcinoma (SCC) immunostained with CAM5.2 (**a,c,e**) and CK19 (**b,d,f**). A primary tumor of the tongue was negative for both cytokeratins (**a,b**). A metastatic lung SCC was also negative for both cytokeratins (**c,d**). Only a primary lung SCC expressed CAM5.2 (**e**) and CK19 (**f**). Scale bars, 300 μm.

Table 6 CAM5.2 and CK19 expression in primary and metastatic sites of tongue squamous cell carcinoma. Note that expression patterns were consistent in 90% (9/10) for CAM5.2 and 70% (7/10) for CK19

	CAM5.2			CK19		
Case	Tongue	Lung	Consistency	Tongue	Lung	Consistency
1	N/A	–	?	N/A	–	?
2	–	–	Yes	–	+	No
3	–	–	Yes	–	–	Yes
4	–	–	Yes	–	–	Yes
5	+	–	No	+	–	No
6	–	–	Yes	–	–	Yes
7	–	–	Yes	–	–	Yes
8	–	–	Yes	–	–	Yes
9	+	+	Yes	–	–	Yes
10	–	–	Yes	–	–	Yes
11	–	–	Yes	–	+	No

–, negative; +, positive; ?, unknown; N/A, not applicable.

CAM5.2 and CK19, CK of columnar epithelium, than primary tumors of the tongue and their metastases. There are two previous reports that are largely in line with our results. The first showed that CK8, 18 and 19, which are characteristic of columnar epithelium, were more frequently expressed in primary SCC of the lung and cervix than in SCC arising from various organs of proper squamous epithelium.[6] The second demonstrated that primary lung SCC express CK19 more frequently and intensely than SCC of the oral cavity.[7] Hamakawa *et al.* reported a somewhat higher value of CK19 reactivity, about 50%, in oral SCC,[7] whereas ours was 2/11 (18%) to 2/15 (13%). This is the result of the generally high reactivity of CK19 in their study, that is 100% strong positivity in primary lung SCC. The high reactivity may be due to: (i) their use of a different antibody and a different augmentation method; (ii) admixture of oral SCC, including those of tongue, gingiva, pharynx and larynx; and (iii) a possible of lack noncancerous controls. We believe our methods are appropriate for detecting heterogeneous reactivity in a tumor.

Our method is highly useful for resected materials, as mentioned above, and it is also applicable for biopsy specimens, provided that pathologists who use this method carefully evaluate the results. Although primary lung SCC frequently express CAM5.2 or CK19, some cases show heterogeneous expression of these markers. Thus, when only a small amount of lung tissue is available, CAM5.2 or CK19 negative studies of biopsy materials do not necessarily mean that the entire tumor is negative for these markers. In such a case, our method would not be helpful for the distinction. However, if a biopsy specimen expresses either CAM5.2 or CK19, the finding will strongly suggest that the lung tumor is a new primary one.

In summary, primary lung SCC express CAM5.2 and CK19 more frequently than do metastatic lung SCC from the tongue. The profiling of these CK could be useful for distinguishing between primary tumors and metastases.

ACKNOWLEDGMENTS

The authors thank Mr Motoyoshi Iwakoshi and Ms Tomoyo Kakita (Division of Pathology, JFCR Cancer Institute) for their technical assistance. There are no conflicts of interests regarding submission of this manuscript.

REFERENCES

1 Carvalho AL, Magrin J, Kowalski LP. Sites of recurrence in oral and oropharyngeal cancers according to the treatment approach. *Oral Dis* 2003; **9**: 112–18.
2 Taneja C, Allen H, Koness RJ, Radie-Keane K, Wanebo HJ. Changing patterns of failure of head and neck cancer. *Arch Otolaryngol Head Neck Surg* 2002; **128**: 324–7.
3 Calhoun KH, Fulmer P, Weiss R, Hokanson JA. Distant metastases from head and neck squamous cell carcinomas. *Laryngoscope* 1994; **104**: 1199–205.
4 Nagle RB, Moll R, Weidauer H, Nemetschek H, Franke WW. Different patterns of cytokeratin expression in the normal epithelia of the upper respiratory tract. *Differentiation* 1985; **30**: 130–40.
5 Ramaekers F, Huysmans A, Moesker O *et al.* Monoclonal antibody to keratin filaments, specific for glandular epithelia and their tumors. Use in surgical pathology. *Lab Invest* 1983; **49**: 353–61.
6 van Dorst EB, van Muijen GN, Litvinov SV, Fleuren GJ. The limited difference between keratin patterns of squamous cell carcinomas and adenocarcinomas is explicable by both cell lineage and state of differentiation of tumor cells. *J Clin Pathol* 1998; **51**: 679–84.
7 Hamakawa H, Bao Y, Takarada M, Fukuzumi M, Tanioka H. Cytokeratin expression in squamous cell carcinoma of the lung and oral cavity: An immunohistochemical study with possible clinical relevance. *Oral Surg Oral Med Oral Pathol Oral Radiol Endod* 1998; **85**: 438–43.
8 Makin C, Bobrow L, Bodmer W. Monoclonal antibody to cytokeratin for use in routine histopathology. *J Clin Pathol* 1984; **37**: 975–83.
9 Moll R, Franke W, Schiller D, Geiger B, Krepler R. The catalog of human cytokeratins: Patterns of expression in normal epithelia, tumors, and cultured cells. *Cell* 1982; **31**: 11–24.
10 Di Como CJ, Urist MJ, Babayan I *et al.* p63 expression profiles in normal and tumor tissues. *Clin Cancer Res* 2002; **8**: 494–501.
11 Effiom OA, Adeyemo WL, Omitola OG, Ajayi OF, Emmanuel MM, Gbotolorun OM. Oral squamous cell carcinoma: A clinicopathologic review of 233 cases in Lagos, Nigeria. *J Oral Maxillofac Surg* 2008; **66**: 1595–9.
12 Lam L, Logan RM, Luke C. Epidemiological analysis of tongue cancer in South Australia for the 24-year period, 1977–2001. *Aust Dent J* 2006; **51**: 16–22.
13 Thun MJ, Lally CA, Flannery JT, Calle EE, Flanders WD, Heath CW Jr. Cigarette smoking and changes in the histopathology of lung cancer. *J Natl Cancer Inst* 1997; **89**: 1580–86.
14 Travis WD, Travis LB, Devesa SS. Lung cancer. *Cancer* 1995; **75**: 191–202.
15 Grønbaek M, Becker U, Johansen D, Tønnesen H, Jensen G, Sørensen TI. Population based cohort study of the association between alcohol intake and cancer of the upper digestive tract. *BMJ* 1998; **317**: 844–7.
16 Macfarlane GJ, Macfarlane TV, Lowenfels AB. The influence of alcohol consumption on worldwide trends in mortality from upper aerodigestive tract cancers in men. *J Epidemiol Community Health* 1996; **50**: 636–9.

Cancer Research

Correlating Phosphatidylinositol 3-Kinase Inhibitor Efficacy with Signaling Pathway Status: *In silico* and Biological Evaluations

Shingo Dan[1], Mutsumi Okamura[1], Mariko Seki[1], Kanami Yamazaki[1], Hironobu Sugita[1], Michiyo Okui[2,3], Yumiko Mukai[1], Hiroyuki Nishimura[4], Reimi Asaka[2], Kimie Nomura[2], Yuichi Ishikawa[2], and Takao Yamori[1]

Abstract

The phosphatidylinositol 3-kinase (PI3K) pathway is frequently activated in human cancers, and several agents targeting this pathway including PI3K/Akt/mammalian target of rapamycin inhibitors have recently entered clinical trials. One question is whether the efficacy of a PI3K pathway inhibitor can be predicted based on the activation status of pathway members. In this study, we examined the mutation, expression, and phosphorylation status of PI3K and Ras pathway members in a panel of 39 pharmacologically well-characterized human cancer cell lines (JFCR39). Additionally, we evaluated the *in vitro* efficacy of 25 PI3K pathway inhibitors in addition to conventional anticancer drugs, combining these data to construct an integrated database of pathway activation status and drug efficacies (JFCR39-DB). *In silico* analysis of JFCR39-DB enabled us to evaluate correlations between the status of pathway members and the efficacy of PI3K inhibitors. For example, phospho-Akt and KRAS/BRAF mutations prominently correlated with the efficacy and the inefficacy of PI3K inhibitors, respectively, whereas *PIK3CA* mutation and PTEN loss did not. These correlations were confirmed in human tumor xenografts *in vivo*, consistent with their ability to serve as predictive biomarkers. Our findings show that JFCR39-DB is a useful tool to identify predictive biomarkers and to study the molecular pharmacology of the PI3K pathway in cancer. *Cancer Res; 70(12); 4982–94. ©2010 AACR.*

Introduction

Phosphatidylinositol 3-kinases (PI3K) are lipid kinases that phosphorylate phosphoinositide at position D3 of the inositol ring (1, 2). The catalytic subunit of class I PI3K is composed of four isoforms (p110α, p110β, p110δ, and p110γ, encoded by *PIK3CA, PIK3CB, PIK3CD*, and *PIK3CG*). Among these isoforms, *PIK3CA* is often activated in cancer by gain-of-function hotspot mutations (3, 4) and gene amplification (5, 6). On the other hand, phosphatase and tensin homologue deleted on chromosome 10 (PTEN) is a lipid phosphatase that dephosphorylates PIP3 at position D3 of the inositol ring to generate PIP2. *PTEN* has been shown to be a tumor suppressor gene and is often inactivated by deletion or mutation in cancer (7–9). Activation of PI3K and PTEN loss trigger sequential phosphorylation of the PI3K downstream signal cascade, including Akt and mammalian target of rapamycin (mTOR), and mediates a survival signal, as well as tumor proliferation (9). Therefore, the PI3K pathway is thought to be a promising therapeutic target.

LY294002 and wortmannin are first-generation PI3K inhibitors, but neither has progressed to clinical trials because of cytotoxicity to liver and skin (10, 11). We previously reported a selective PI3K inhibitor, ZSTK474, which has potent antitumor activity and low toxicity *in vivo* (12). Subsequently, several PI3K inhibitors have been developed, and some including NVP-BEZ235 and GDC-0941 have already entered clinical trials (13–15). In addition to PI3K inhibitors, antitumor compounds targeting Akt and mTOR have been developed (15–18).

To develop a molecular-targeted anticancer drug, it is highly desirable to develop predictive biomarkers for stratifying patients susceptible to the drug. In fact, mutations of *EGFR* and *KRAS* are used to predict the efficacy of gefitinib in lung cancer and that of cetuximab in colorectal cancer, respectively (19–22). Moreover, Engelman and colleagues recently showed that tumor growth triggered by KRAS mutant exhibited resistance to NVP-BEZ235 (23). On the other hand, dysregulation of *PIK3CA* and PTEN has been reported to be involved in resistance to EGFR-targeted therapies (24–26). As mentioned above, *PIK3CA* mutation and PTEN loss trigger

Authors' Affiliations: [1]Division of Molecular Pharmacology, Cancer Chemotherapy Center, and [2]Department of Pathology, Cancer Institute, Japanese Foundation for Cancer Research, Tokyo, Japan and [3]Department of Biomedical Engineering, Toin Human Science and Technology Center, and [4]Department of Biomedical Engineering, Toin University of Yokohama, Yokohama, Japan

Note: Supplementary data for this article are available at Cancer Research Online (http://cancerres.aacrjournals.org/).

Corresponding Author: Takao Yamori, Division of Molecular Pharmacology, Cancer Chemotherapy Center, Japanese Foundation for Cancer Research, 3-8-31 Ariake, Koto-ku, Tokyo 135-8550, Japan. Phone: 81-3-3520-0111 ext. 5432; Fax: 81-3570-0484; E-mail: yamori@jfcr.or.jp.

doi: 10.1158/0008-5472.CAN-09-4172

activation of the kinase cascade of the PI3K downstream pathway. However, it is not well understood whether the efficacy of PI3K pathway inhibitors could be predicted by these upstream abnormalities and downstream activities of the PI3K pathway.

We previously established a panel of 39 human cancer cell lines (JFCR39) derived from various organs (27–29). JFCR39, as well as NCI60 developed by National Cancer Institute, has been used as an *in vitro* tool to measure "fingerprints" of cytotoxic compounds. Fingerprints are defined as the patterns of differential drug efficacy across a panel of cell lines and have been found to reflect mechanisms of drug action (27–30). ZSTK474 is a compound that we identified as a new PI3K inhibitor based on the similarity with the fingerprint of LY294002 (12). In other words, each of the JFCR39 cell lines showed similar responses to ZSTK474 and LY294002, and the responses varied from cell line to cell line. This suggested that the status of biological pathways determining a cancer cell's response to PI3K inhibitors (which may include the PI3K pathway) is heterogeneous across these cell lines.

In the present study, taking advantage of JFCR39, we examined the mutation and/or expression of upstream regulators of the PI3K and Ras pathways, including four PI3K isoforms (*PIK3CA, PIK3CB, PIK3CD*, and *PIK3CG*), *PTEN*, the ERBB family receptor tyrosine kinases (RTKs), *KRAS* and *BRAF*, and the phosphorylation of downstream pathway members including Akt, TSC2, GSK-3, mTOR, S6K1, mitogen-activated protein kinase (MAPK)/extracellualr signal-regulated kinase (ERK) kinase (MEK)-1/2, and ERK1/2. Next, we examined the fingerprints of 25 compounds targeting the PI3K pathway as well as other conventional anticancer drugs. We then combined the PI3K and Ras pathway database and the drug database to develop an integrated database of pathway status and drug efficacies (JFCR39-DB). Using this database, we first evaluated the functional relationships among these pathway inhibitors and those among drugs by comparing their fingerprints. Second, we evaluated the correlation between PI3K pathway members and PI3K pathway inhibitors to identify candidate biomarkers for predicting their efficacy.

Materials and Methods

Cell lines and cell culture

A panel of 39 human cancer cell lines, termed JFCR39, were previously described (27, 28, 31). Cells were grown in RPMI 1640 (Wako Pure Chemical Industries Ltd.) supplemented with 1 μg/mL kanamycin and 5% (v/v) fetal bovine serum (Moregate Exports) and incubated at 37°C in a humidified atmosphere supplemented with 5% CO_2. Authentication of cell lines was done by short tandem repeat analysis using PowerPlex16 Systems (Promega; data not shown).

Amplification of genomic DNA fragments for sequencing

Extraction of genomic DNA was done using DNeasy blood and tissue kit (Qiagen) according to the manufacturer's instructions. Amplification of genomic DNA fragments was done using Pfu Ultra High-Fidelity DNA polymerase (Agilent Technologies), FastStart High Fidelity PCR System (Roche Applied Science), or AccuPrime Taq DNA Polymerase High Fidelity (Invitrogen). Polymerases and primer sequences used in each reaction are shown in Supplementary Table S1.

Nucleotide sequence analysis

Sequencing reactions were done using BigDye Terminator v3.1 and dGTP BigDye Terminator v3.0 (Applied Biosystems) according to the manufacturer's instructions. Primers were shown in Supplementary Table S1. Nucleotide sequences were analyzed using a 3130 Genetic Analyzer (Applied Biosystems) and sequence files were edited using 4 Peaks software (Mekentosj B.V.).

Detection of lipid kinase activities of PI3K p110α mutants

Determination of lipid kinase activities of PI3K p110α was described as previously (32). In brief, HEK293T cells were transfected with pFLAG-PIK3CA (with or without mutation) and pc-PIK3R1 using Lipofectamine 2000 (Invitrogen). After 48 hours of incubation, cells were harvested and the lysates were immunoprecipitated by using FLAG-Tagged Protein Immunoprecipitation Kit (Sigma-Aldrich). To detect kinase activity, we used the PI3K-HTRF assay kit (Millipore) and EnVision 2103 Mutilabel Reader (Perkin-Elmer).

Preparation of total cell extract

Cells were resuspended in lysis buffer [10 mmol/L Tris-HCl (pH 7.4)], 50 mmol/L NaCl, 0.5% w/v NP40, 0.1% w/v SDS, 50 mmol/L sodium fluoride, 30 mmol/L sodium pyrophosphate, 50 mmol/L sodium orthavanadate, 5 mmol/L EDTA, 0.1 trypsin inhibitor unit/mL aprotinin, and 1 mmol/L phenylmethylsulfonyl fluoride] and lysed by sonication in an ice bath. Concentrations of proteins in the extracts were determined using a protein assay kit (Pierce).

Immunoblot analysis

Equal amounts of protein were subjected to SDS-PAGE and the separated proteins were transferred onto an Immobilon FL polyvinylidene difluoride membrane (Millipore). The membrane was incubated with a primary antibody. The antibodies for PI3K p110α, Akt, phospho-Akt (T308, S473), phospho-GSK-3 (S9), phospho-TSC2 (T1462), phospho-mTOR (S2448), phospho-S6K1 (T389), phospho-MEK1 (S217/S221), and phospho-ERK1/2 (T202/Y204) were purchased from Cell Signaling Technologies. The antibodies for PI3K p110β, p110γ, and p110δ were purchased from Millipore. The antibody for PTEN was purchased from BD Biosciences Pharmingen. Bound antibody was quantitatively detected using an appropriate antimouse or rabbit immunoglobulin secondary antibody labeled with Alexa Fluor 680 (Invitrogen) and the Odyssey Infrared Imaging System (LI-COR). Data shown are median values of three independent experiments.

Table 1. Missense mutations of PI3K isoforms, *PTEN*, *KRAS*, and *BRAF* in JFCR39

ID	Origin	Cell line	*PIK3CA*	*PIK3CB*	*PIK3CD*	*PIK3CG*	*PTEN*	*KRAS*	*BRAF*
01	Lung ca.	NCI-H23				P538L		G12C	
02		NCI-H226				S442Y (SNP)			
03		NCI-H522							
04		NCI-H460	E545K (genomic)					Q61H	
05		A549						G12S	
06		DMS273				M259I	K128N		
07		DMS114							
11	Colorectal ca.	HCC2998	I391M (SNP)	R149Q R562Q		T857A R273H L466M	Y46C R130Q F341V	A146T	
12		KM-12					G129* K267fs(del.-1)*9		
13		HT-29	P449T			S442Y(SNP)			V600E
15		HCT-15	E545K D549N	R628Q	S174L			G13D	
16		HCT-116	H1047R		Ex.16 del.		G13D		
21	Gastric ca.	St-4				S442Y(SNP)	E291*	G12A	
22		MKN1	E545K						
23		MKN7			T456A (SNP)	A621S			
24		MKN28			T456A (SNP)	A621S			
25		MKN45							
26		MKN74			T456A (SNP)	A621S			
31	Breast ca.	HBC-4		E1051K		S442Y(SNP)			
32		BSY-1	H1047R				Ex.1-9 del.		
34		HBC-5							
35		MCF-7	E545K			S442Y(SNP)			
36		MDA-MB-231						G13D	G464V
41	Ovarian ca.	OVCAR-3							
42		OVCAR-4							
43		OVCAR-5						G12V	
44		OVCAR-8				N522S			
45		SK-OV-3	H1047R						
51	Brain ca.	U251					E242fs(ins.+2)*15		
52		SF-268							
53		SF-295			S312C		R233*		
54		SF-539					Ex.1-9 del.		
55		SNB-75							
56		SNB-78	L719F				T26fs(SD del.)		
61	Renal ca.	RXF-631L				S442Y(SNP)			
62		ACHN							
71	Melanoma	LOX-IMVI							V600E
91	Prostate ca.	DU-145		A686T		S442Y(SNP)			
92		PC-3			S312C	S442Y(SNP)	Ex.3-9 del.		
Total # (without SNP)			10 (9)	4	7 (4)	15 (7)	10	9	3

NOTE: Underline indicates a homozygous mutation.

Drugs

ZSTK474 was kindly provided by Zenyaku Kogyo Co. Ltd. LY294002, PI103, PI3Kα inhibitor IV, PI3Kγ inhibitor (AS605240), and Akt inhibitors II, III, IV, V (triciribine), VIII, IX, X, and XI were purchased from Calbiochem. TGX221 and perifosine were purchased from Cayman. GDC-0941 and IC87114 were obtained from Symansis. RAD001 and CCI779 were purchased from LC Laboratories. Wortmannin,

PX-866, NVP-BEZ235, and rapamycin were obtained from Kyowa Medex, Sigma, Selleck, and Wako Pure Chemical, respectively.

Determination of drug efficacy

Drug efficacy was assessed as changes in total cellular protein after 48 hours of drug treatment using a sulforhodamine B assay. Assays were done in duplicate and the GI_{50} was calculated as described previously (27, 33).

Animal experiments

Animal care and treatment were done in accordance with the guidelines of the animal use and care committee of the Japanese Foundation for Cancer Research and conformed to the NIH Guide for the Care and Use of Laboratory Animals. Female nude mice with BALB/c genetic backgrounds were purchased from Charles River Japan. Mice were maintained under specific pathogen-free conditions and provided with sterile food and water *ad libitum*. Human tumor xenografts were generated by s.c. inoculating nude mice with 3 mm × 3 mm × 3 mm tumor fragments of human cancer cells. When the tumors became 100 to 300 mm^3 in size, ZSTK474 was p.o. administered at 100, 200, and 400 mg/kg of body weight following the indicated schedule. The length (L) and width (W) of the subcutaneous tumor mass were measured by calipers in live mice, and the tumor volume (TV) was calculated as $TV = (L \times W^2)/2$. Percent treated/control [T/C (%)] was calculated as $(TV_{with\ drug}/TV_{control}) \times 100$. To assess toxicity, we measured the body weight of the tumor-bearing mice. Mice were finally sacrificed and tumors were excised and frozen in liquid N_2.

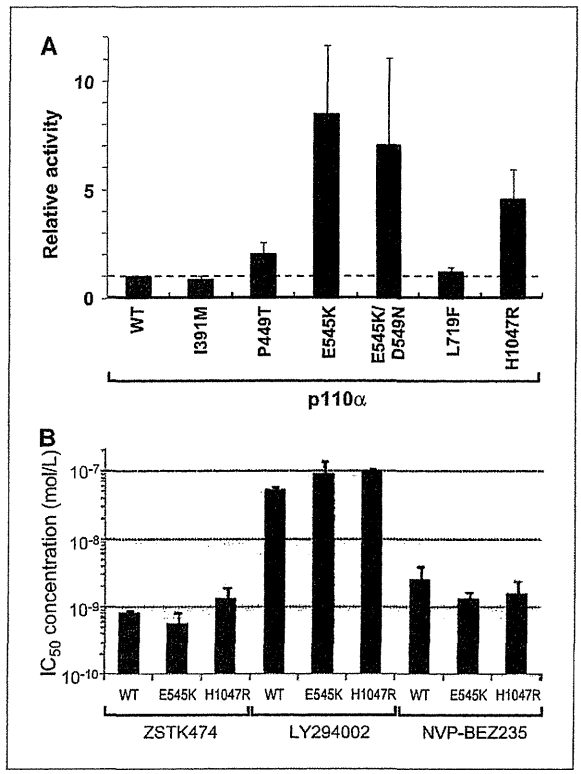

Figure 1. Relative kinase activities of p110α mutants and the inhibitory effect of PI3K inhibitors against hotspot mutants of p110α. A, recombinant FLAG-tagged PI3K p110α/p85α protein complex produced in 293T cells was immunoprecipitated, and the immunoprecipitates were used for the quantitative PI3K-HTRF assay (32). B, effect of three PI3K inhibitors (ZSTK474, LY294002, and NVP-BEZ235) on the enzymatic activity of two hotspot mutants (E545K and H1047R) p110α compared with the wild-type. No striking difference was observed in the IC_{50} concentrations of these inhibitors between wild-type and mutant p110α.

Results

Characterization of the mutation status of PIK3Cs, PTEN, KRAS, and BRAF in JFCR39 cell lines

We first examined the mutation status of PI3K isoforms in the JFCR39 cell lines (Table 1; Supplementary Table S2). Analysis of genomic sequences of *PIK3CA* on exon 9 and exon 20 revealed the hotspot mutations (E545K in four cell lines and H1047R in three cell lines). Analysis of the full coding sequence of cDNA revealed four additional missense mutations: I391M, P449T, D549N, and L719F. Evaluation of relative kinase activity of these mutants revealed that mutant P449T exhibited gain of function (>2-fold) compared with wild-type PI3Kα (Fig. 1A). The E545K mutation found in NCI-H460 genomic DNA was not detected in the cDNA, suggesting that the allele with the E545K mutation was hardly transcribed in NCI-H460 cells. Therefore, we concluded that seven cell lines [HCT-116, SK-OV3, BSY-1 (H1047R), MKN-1, MCF7 (E545K), HCT-15 (E545K/D549N), and HT-29 (P449T)] expressed a gain-of-function mutant of *PIK3CA*. With regard to two hotspot mutants (E545K and H1047R), we examined the effect of three representative PI3K inhibitors on their enzymatic activity and found no striking difference in their efficacies compared with wild-type p110α (Fig. 1B).

In addition to *PIK3CA*, we examined the genomic sequences of all coding exons of *PIK3CB*, *PIK3CD*, and *PIK3CG* genes and found five missense mutations in *PIK3CB*, three in *PIK3CD*, and eight in *PIK3CG* (Table 1; Supplementary Table S2). Most of these mutations were not registered in the dbSNP database established by The National Center for Biotechnology Information. Therefore, this study is the first report showing that cancer cells harbor missense mutations in *PIK3CB*, *PIK3CG*, and *PIK3CD* as well as in *PIK3CA*.

Next, we proceeded to examine the genomic sequences of the *PTEN* gene and found that the *PTEN* gene was deleted in three cell lines (BSY-1, SF539, and PC-3), and seven had missense or frameshift mutations.

We examined the genomic sequences of exon 1 (including G12 and G13) and exon 2 (Q61) of *KRAS* and exon 15 (V600) and exon 11 (G464, G466, and G468) of *BRAF* (Table 1). Eight of 39 cell lines had a hotspot mutation in the G12, G13, or Q61 residue. On the other hand, the *BRAF* mutation was observed in three cell lines including LOX-IMVI.

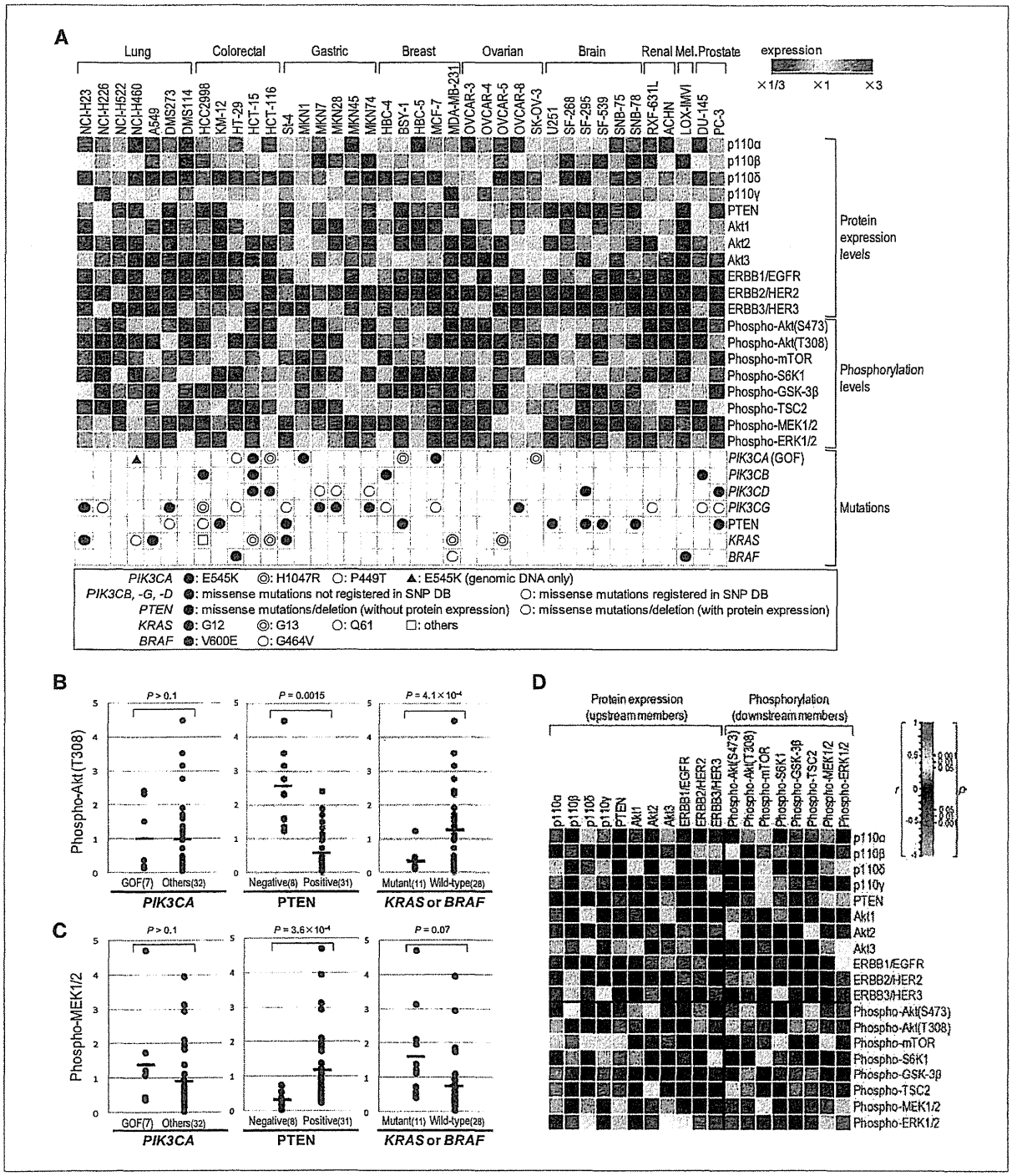

Figure 2. Mutation, protein expression, and phosphorylation status of PI3K and Ras pathway members and the correlation among them. A, the protein expression of upstream members and the phosphorylation of downstream members in each of the JFCR39 cell lines were determined by immunoblot analysis and normalized so that their average across the JFCR39 cell lines was 1 (yellow). A red point and a blue point represent high and low expression by 3-fold, respectively. Mutation data are from Table 1. B and C, differences in expression levels of phospho-Akt (T308) (B) and phospho-MEK1/2 (C) between cell lines with or without *PIK3CA* gain-of-function mutation (GOF), PTEN expression, and *KRAS/BRAF* mutation. Student's *t* tests were used to examine significance of differential expression. D, a heat map representing the similarities among the fingerprints of PI3K pathway members. Red to yellow: significant positive correlation ($P < 0.05$); yellow to black, black to blue: no significant correlation ($P > 0.05$), blue to sky blue: significant negative correlation ($P < 0.05$).

Expression of PI3K isoforms, PTEN, Akt isoforms, and ERBB-family RTKs

We next examined the protein expression of upstream members of the *PI3K* pathway that would affect downstream activity, including PI3K isoforms (p110α/β/γ/δ), PTEN, Akt isoforms (Akt1/2/3), and ERBB-family RTKs (EGFR/ERBB2/ERBB3; Fig. 2A; Supplementary Data). As expected, p110α and p110β were widely expressed, whereas p110γ and p110δ, which were thought to be expressed preferentially in leukocytes, were unexpectedly expressed in most JFCR39 cell lines derived from solid tumors. PTEN expression was undetectable in all of three cell lines with the deletion and in five of seven cell lines with a mutation, whereas all of 29 cell lines lacking a mutation or deletion expressed a certain amount of PTEN protein (Supplementary Fig. S1). Some of the cell lines exhibited overexpression of Akt isoforms; SF268 and MCF-7 highly expressed Akt1, whereas OVCAR3 and HBC5 highly expressed Akt2. EGFR was expressed in a wide variety of cell lines, but in some cell lines including NCI-H522 and MCF-7, EGFR expression was absent or present at an extremely low level. ERBB3 was highly expressed in a wide variety of cell lines derived from ovarian, gastric, breast, and colorectal cancer cell lines, but not in most brain cancer cell lines. On the other hand, ERBB2 was highly expressed in two cell lines (SK-OV-3 and HBC5).

Activation status of downstream members of the PI3K pathway

We examined the phosphorylation levels of PI3K downstream effectors including Akt (phosphorylated on T308 and S473), mTOR (S2448), S6K1 (T389), GSK-3β (S9), and TSC2 (T1462; Fig. 2A). We also examined Ras downstream effectors, phosphorylated MEK1/2 (S217/S221) and ERK1/2 (T202/Y204). Interestingly, the expression pattern of phosphorylated Akt (T308) was highly correlated with phosphorylated TSC2 ($r = 0.70$) and GSK-3β ($r = 0.60$), but not with phosphorylated mTOR and S6K1 (Fig. 2A; Supplementary Fig. S2). On the other hand, expression levels of phosphorylated Akt (T308) had a significant negative correlation with phosphorylated ERK1/2 ($r = 0.39$).

Correlation between upstream abnormalities and phosphorylation of downstream effectors in the PI3K pathway

Correlation analysis between upstream abnormalities and downstream activities revealed some interesting results (Fig. 2B and C; Supplementary Table S3). For example, phosphorylation levels of Akt (T308) ($P = 0.0015$) and TSC2 ($P = 0.011$) were significantly higher and those of MEK1/2 ($P = 3.6 \times 10^{-4}$) and ERK1/2 ($P = 2.7 \times 10^{-5}$) were significantly lower in eight PTEN-negative cell lines than those in 31 PTEN-expressing cell lines. This suggested that PTEN loss conferred activation of PI3K downstream factors and inactivation of the MAPK pathway. In contrast, phosphorylation levels of Akt (T308) ($P = 4.1 \times 10^{-4}$) and TSC2 ($P = 0.0021$) were significantly lower in cell lines having a mutation in either the *KRAS* or the *BRAF* gene, suggesting inactivation of the PI3K/Akt pathway in these cell lines. However, mutation of *PIK3CA* did not have significant associations with downstream activation, including phosphorylation levels of Akt and MEK.

Determination of efficacy patterns of 25 PI3K pathway inhibitors across JFCR39 cell lines, or fingerprints, and evaluation of their modes of action from their fingerprints

We next examined the efficacy of 25 PI3K pathway inhibitors (Table 2) in each of the JFCR39 cell lines. Then, we compared the fingerprints of PI3K inhibitors with those of other conventional anticancer drugs by cluster analysis (Fig. 3A; Supplementary Fig. S3A). Interestingly, 10 of 11 PI3K inhibitors were tightly clustered and the cluster also included Akt inhibitor VIII (AKTi-1/2) and rapamycins, suggesting similarity in the mechanisms of action across these compounds. Moreover, their fingerprints were clearly different from those of the remainder of the 10 Akt inhibitors, all of three MEK inhibitors, and other conventional anticancer drugs. Furthermore, comparison of the fingerprints of 15 PI3K pathway inhibitors in the cluster revealed that some pairs, including ZSTK474/GDC-0941 ($r = 0.86$), wortmannin/PX-866 ($r = 0.81$), and PI103/PI3Kα inhibitor IV ($r = 0.80$), exhibited extremely high correlations, suggesting a close similarity in the molecular mechanisms of action between each pair of compounds (Supplementary Fig. S3B–D).

Construction of an integrated database and correlations between the status of pathway members and the efficacy of PI3K inhibitors

We have thus far studied the drug efficacy data and the signal pathway data with regard to JFCR39 cell lines. We then combined these data to develop an integrated database (JFCR39-DB). Using JFCR39-DB, we studied the relationship between the activation status of the PI3K pathway and the efficacy of PI3K pathway inhibitors. First, we examined the correlation between the mutation status of upstream members and drug efficacy. The Student *t* test revealed no significant differences in the efficacies of all of 25 PI3K pathway inhibitors examined, in seven cell lines expressing a gain-of-function mutant of PI3Kα, and in the remainder of the 32 cell lines (Fig. 3B; Supplementary Table S4). As mentioned before, we examined the effect of three representative PI3K inhibitors on the enzymatic activity of two hotspot mutants of PI3Kα and found no striking difference in their efficacies compared with wild-type p110α (Fig. 1B). These results suggest that cancer cells expressing mutant PI3Kα are susceptible to PI3K inhibitors to a similar extent as those expressing wild-type PI3Kα. Moreover, PTEN status did not correlate with the efficacy of PI3K pathway inhibitors. In addition, the mutation status of other PI3K isoforms did not exhibit striking correlations either. On the other hand, cell lines having a mutation in either *KRAS* or *BRAF* exhibited resistance to several PI3K pathway inhibitors including ZSTK474 (Fig. 3B; Supplementary Table S4). The present results suggest that *KRAS/BRAF*

Table 2. The 25 PI3K pathway inhibitors used in this study and their profiles and structures (15–18)

PI3K inhibitors

ZSTK474 (4.8×10^{-7} mol/L) Selective PI3K inhibitor Preclinical	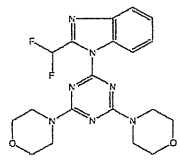	Wortmannin (9.7×10^{-6} mol/L) PI3K/mTOR/MLCK inhibitor Preclinical	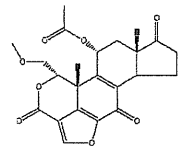	LY294002 (8.1×10^{-6} mol/L) PI3K/mTOR/CK2 inhibitor Preclinical	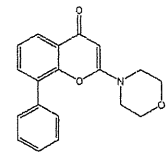
PI103 (1.8×10^{-7} mol/L) PI3K/mTOR inhibitor Preclinical	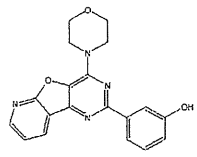	PX866 (1.4×10^{-6} mol/L) PI3Kα/δ/γ inhibitor; derivative of wortmannin Phase I	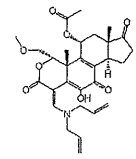	NVP-BEZ235 (8.6×10^{-9} mol/L) PI3K/mTOR inhibitor Phase I/II	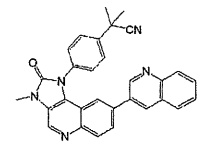
GDC-0941 (5.0×10^{-7} mol/L) Selective PI3K inhibitor Phase I	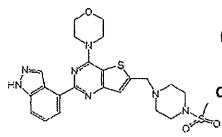	PI3Kα inhibitor IV (1.0×10^{-6} mol/L) PI3Kα/β inhibitor; derivative of PI103 Preclinical	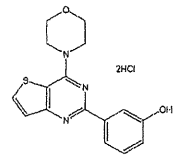	TGX221 (1.0×10^{-5} mol/L) Selective PI3Kβ inhibitor Preclinical	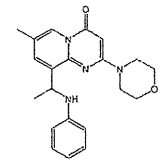
IC87114 (CAL-101; 8.3×10^{-5} mol/L) Selective PI3Kδ inhibitor Phase I	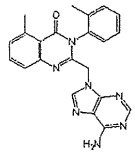	AS605240 (PI3Kγ inhibitor; 9.5×10^{-6} mol/L) Selective PI3Kγ inhibitor Preclinical	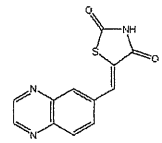		

Akt inhibitors

Deguelin (7.6×10^{-6} mol/L) Selective Akt inhibitor; derivative of rotenone Preclinical	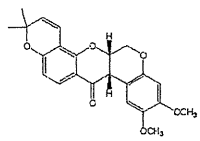	Perifosine (9.1×10^{-6} mol/L) Lipid-based PI analogue Phase II	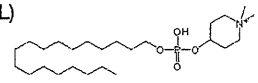	Akt inhibitor (1.3×10^{-5} mol/L) Lipid-based PI analogue Preclinical	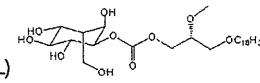
Akt inhibitor II (8.6×10^{-6} mol/L) Lipid-based PI analogue Preclinical	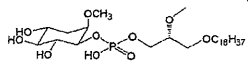	Akt inhibitor III (1.9×10^{-5} mol/L) Lipid-based PI analogue Preclinical	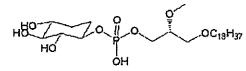	Akt inhibitor IV (2.8×10^{-7} mol/L) Preclinical	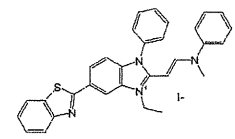
Akt inhibitor V (triciribine/ VQD-002; 2.2×10^{-5} mol/L) Tricyclic nucleotide Phase I/II (as triciribine phosphate)	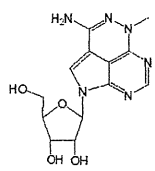	Akt inhibitor VIII (AKTi-1/2; 8.6×10^{-6} mol/L) Allosteric Akt1/2 inhibitor Preclinical	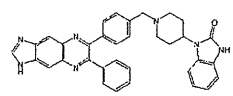	Akt inhibitor IX (8.0×10^{-7} mol/L) Preclinical	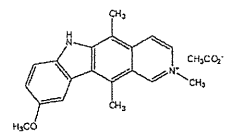

(*Continued on the following page*)